induced anti-HCV replicon activity was time dependent (Fig. 1b). GGA was combined with IFN-α to examine the additive effect (Fig. 1c). One or 10 μmol/L of GGA combined with IFN-α decreased the relative *Renilla* luciferase activity slightly (Fig. 1c). However, 50 or 100 μmol/L of GGA combined with IFN-α decreased the relative *Renilla* luciferase activity with statistical difference. GGA treatment did not have any statistically significant effect on cell viability from 1 to 100 μmol/L of GGA for 24 h (data not shown).

GGA did not activate the tyrosine-701 and serine-727 on STAT-1, and did not induce PKR and HSP-70 in OR6 cells

GGA mediated phosphorylation of STAT-1 at the tyrosine-701 and serine-727 residues was investigated using antibodies to phospho-specific STAT-1 on OR6 cells. No phosphorylation of tyrosine-701 and serine-727 on STAT-1 was detected in OR6 cells (Fig. 2a). IFN induce anti-viral

protein, PKR, and STAT-1 has an interferon stimulating responsive element (ISRE) in the promoter region [12]. The expression levels of both proteins did not change throughout this study, as indicated by a Western blotting analysis (Fig. 2b, c). Next, the role of HSP in the mechanism of GGA activity was examined because GGA is an inducer of HSP. The HSP-70 expression was increased by pre-exposure to heat shock (Fig. 2d, lanes 2, 4), but it did not increase due to the effects of GGA (Fig. 2d, lanes 3, 4).

Rapamycin and mTOR specific siRNA, but not PI3-K inhibitor and Akt inhibitor, were able to cancel the GGA induced anti-HCV activity

The role of the PI3-K-Akt-mTOR pathway the anti-HCV activity of GGA was examined in OR6 cells. The cells were treated with GGA after 3 h in the presence or absence of rapamycin as an mTOR inhibitor, Akt inhibitor, or wortmannin as a PI3-K inhibitor (Fig. 3). Pretreatment with rapamycin attenuated the anti-HCV replication effect
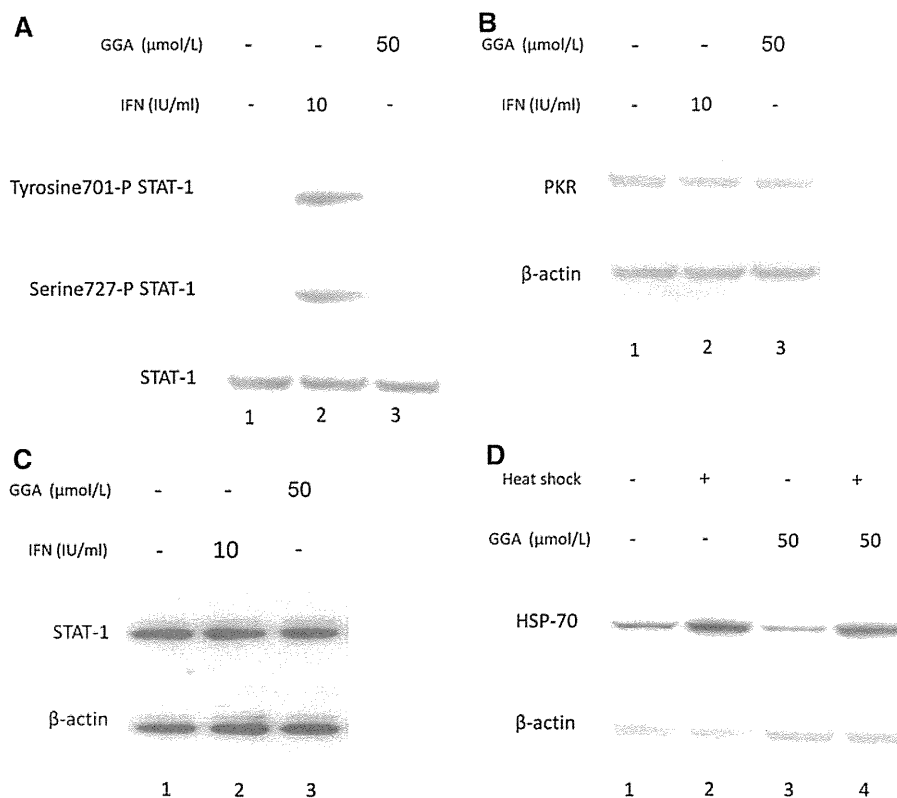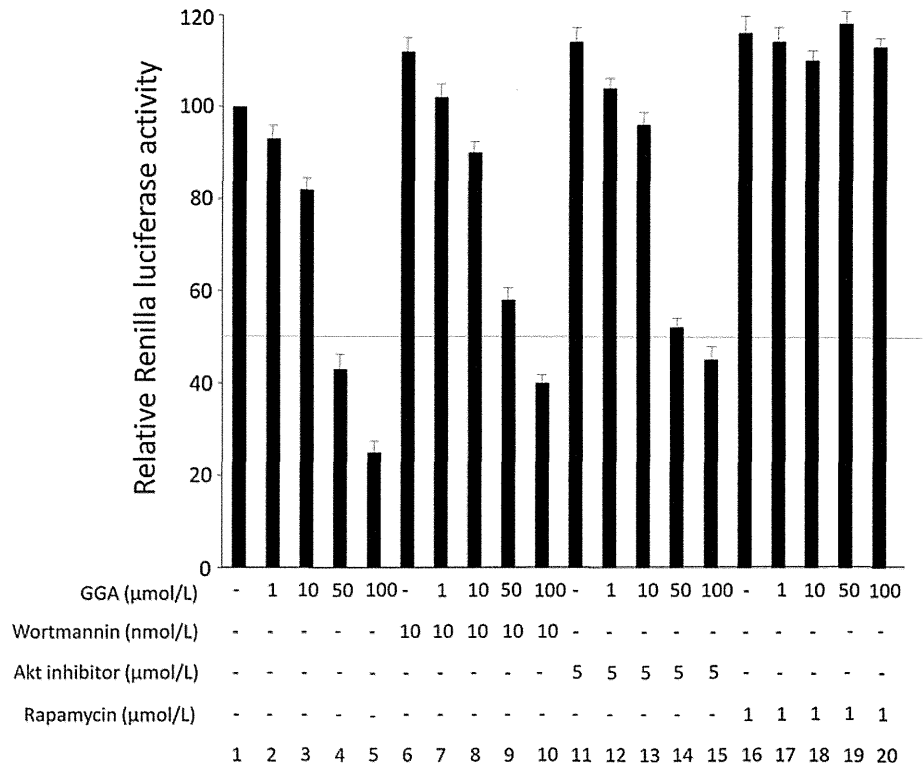

Fig. 2 Effect of GGA on STAT-1 (**a**), PKR (**b**) and HSP-70 (**c**). **a** The OR6 cells were either untreated (*lane 1*) or treated with 10 IU/mL of IFN-α (*lane 2*) for 30 min or treated with 50 μmol/L GGA (*lane 3*) and then were phosphorylated STAT-1 at tyrosine-701 residue (*upper panel*) and at serine-727 residue (*middle panel*), the expression STAT-1 (*lower panel*) was analyzed by Western blotting. **b** The OR6 cells were either untreated (*lane 1*) or treated with 10 IU/mL of IFN-α (*lane 2*) for 30 min or treated with 50 μmol/L GGA (*lane 3*),

and then the expression of PKR (*upper panel*) was analyzed by a Western blotting analysis. The β-actin (*lower panel*) protein expression was used as an internal control. **c** The OR6 cells were either untreated (*lane 1*) or given heat shock (at 42°C 15 min, overnight recovery at 37°C) (*lanes 2, 4*) or treated with 50 μmol/L of GGA (*lanes 3, 4*) and then the expression HSP-70 (*upper panel*) was analyzed by Western blotting. β-Actin (*lower panel*) protein is the internal control

Fig. 3 Changes in GGA suppressed HCV replication by rapamycin, but not PI3-K inhibitor and Akt inhibitor. OR6 cells were treated with 1–100 μmol/L of GGA in the absence (*lanes 2–5*) or presence of pretreatment (*lanes 7–10, 12–15, 17–20*) for 3 h. *Lanes 1, 6, 11* and *16* were not treated with GGA. *Lanes 6, 11* and *16* were treated with wortmannin, an Akt inhibitor, and rapamycin, respectively. One day later, *Renilla* luciferase activity was determined by luminometer (*n* = 4). The data are expressed as the mean ± SD and are representative of four similar experiments

GGA (μmol/L)	-	1	10	50	100	-	1	10	50	100	-	1	10	50	100	-	1	10	50	100
Wortmannin (nmol/L)	-	-	-	-	-	10	10	10	10	10	-	-	-	-	-	-	-	-	-	-
Akt inhibitor (μmol/L)	-	-	-	-	-	-	-	-	-	-	5	5	5	5	5	-	-	-	-	-
Rapamycin (μmol/L)	-	-	-	-	-	-	-	-	-	-	-	-	-	-	-	1	1	1	1	1
	1	2	3	4	5	6	7	8	9	10	11	12	13	14	15	16	17	18	19	20

in comparison to GGA alone (Fig. 3, lanes 17–20), whereas pretreatment with wortmannin and Akt inhibitor did not increase the *Renilla* luciferase activity (Fig. 3, lanes 7–10, 12–15). siRNA transfection was used for mTOR knockdown to explore role of mTOR in the anti-HCV activity (Fig. 4). The transfection efficiency of the siRNA was confirmed by a Western blotting analysis. In this experiment, the detectable band intensities were quantified by the National Institutes of Health image software program. Although the transfection efficiency of siRNA was barely 46% (Fig. 4a), GGA-induced anti-HCV activity was clearly inhibited in mTOR-siRNA transfected cells (Fig. 4b, lane 4, 6) in comparison to the control cells (Fig. 4b, lanes 3, 5).

GGA induced mTOR activity, mTOR phosphorylation and p70S6K phosphorylation in OR6 cells

The phosphorylation of the serine-2448 residues of mTOR by 50 μmol/L of GGA was detected 30 min after GGA treatment. The band intensity of serine-2448 phosphorylated mTOR decreased by pretreatment with rapamycin but was almost same as with GGA alone following pretreatment with LY294002 (Fig. 5a). Furthermore, an mTOR activity assay was conducted to confirm the activity mechanism of GGA (Fig. 5b). The mTOR activity was increased by treatment with GGA alone (Fig. 5b, lane 4) and was inhibited by pretreatment with rapamycin (Fig. 5b,

lane 6), whereas pretreatment with LY94002 did not suppress the mTOR activity (Fig. 5b, lane 5). Furthermore, to evaluate the mTOR activity, we investigated the level of phospholylated-p70S6K by a Western blotting analysis (Fig. 5c). The phosphorylation of the threonine-389 residue of p70S6K by 50 μmol/L of GGA was detected. Similar to mTOR, the band intensity of phospho-threonine-389 of p70S6K decreased after pretreatment with rapamycin, but the intensity was almost the same as that seen following treatment with GGA alone after pretreatment with LY294002 (Fig. 5c).

Discussion

GGA demonstrated the anti-HCV activity in this study. The anti-HCV effect depended on the GGA induced mTOR activity, not STAT-1 activity. An additive effect was observed with the combination of IFN and GGA.

GGA is a non-toxic heat shock protein (HSP) 70 inducer [13]. Various GGA activities outside of the stomach are also related to HSP induction [14–16]. GGA induced HSP-70 exerts an anti-ischemic stress activity in the heart and liver [16, 17], an anti-inflammatory activity in various cell types [18] and promotes liver regeneration [19]. GGA induces thioredoxin as well as HSP-70 in hepatocytes and other cells [20]. Thioredoxin anti-virus activity, is induced by AP-1 and NF-κB but not HSP-70 [21]. GGA has potent
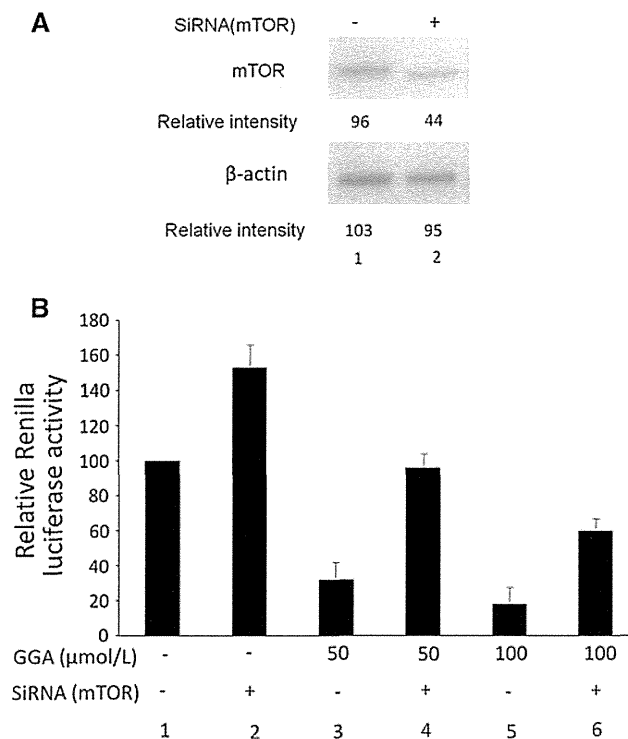
Fig. 4 Changes in GGA suppressed HCV replication by mTOR-siRNA. **a** OR6 cells were transfected with mTOR-siRNA (*lane 1*) or the non-targeted siRNA (*lane 2*). The expression of mTOR was evaluated by a Western blotting analysis. **b** The OR6 cells were transfected with mTOR-siRNA (*lanes 2, 4* and *6*) and the non-targeted siRNA (*lanes 1, 3* and *5*). One day later, the cells were treated with GGA (*lanes 3–6*). The HCV replicon assay is the same as Fig. 3. Non-treatment OR6 cells has 100% of relative *Renilla* luciferase light unit. The *Renilla* luciferase activity increased in the OR6 cells transfected with mTOR-siRNA (*lane 2*) in comparison to the non-targeted siRNA (*lane 1*). However, in OR6 cells treated with GGA, there was a greater elevation of *Renilla* luciferase activity in OR6 cells transfected with mTOR-siRNA (*lanes 4* and *6*) as compared to that with the non-targeted siRNA (*lanes 3* and *5*). The data are expressed as the mean ± SD and are representative example of four similar experiments

antiviral activity via the enhancement of antiviral factors and can clinically provide protection from influenza virus infection [22]. GGA significantly inhibits the synthesis of influenza virus-associated proteins and prominently enhances the expression of human myxovirus resistance 1 (MxA) followed by increased HSP-70 transcription [22]. Moreover, GGA augments the expression of an interferon-inducible double-strand RNA-activated protein kinase (PKR) gene and promotes PKR autophosphorylation and concomitantly alpha subunit of eukaryotic initiation factor 2 phosphorylation during influenza virus infection [22]. These anti-virus activities are related to GGA induced HSP-70. But, HSP-70 protein and PKR were not induced by GGA in OR6 cells in the current study. There is apparently no relationship between the GGA induced anti-

HCV activity and HSP, PKR in OR6 cells. Therefore, we thought that HSP and PKR-independent anti-HCV activity induced by GGA was present in this hepatoma-derived cell line.

GGA induction of anti-viral protein is dependent upon STAT-1 tyrosine phosphorylation in HuH-7 and HepG2 [10]. However, GGA did not induce STAT-1 tyrosine phosphorylation and anti-virus protein, PKR, in OR6 cells in this study. Moreover, the GGA induced anti-HCV activity depended on mTOR activity, not STAT-1. OR6 cells are full length HCV replicon transfected HuH-7 cells [11]. HCV virus products inhibit the Jak-STAT pathway [23–25]. The mechanism of inhibition of the Jak-STAT pathway is multi-factorial including the suppressor of cytokine signaling 3 (SOCS-3) expression [26], protein phosphatase 2A (PP2A) induction [27], STAT-3 expression [28] and IL-8 expression [29]. GGA induced STAT-1 tyrosine phosphorylation and inducible PKR protein levels are also minor. Generally, the replicon transfection induces the intrinsic IFN [30], but STAT-1 tyrosine phosphorylation was not detected in combined OR6 cells. HCV replicon produced viral product might be inhibiting GGA-induced STAT-1 tyrosine phosphorylation.

mTOR is associated with the IFN induced anti-HCV signal [31]. The IFN activated mTOR pathway exhibits important regulatory effects in the generation of the IFN responses, including the anti-encephalomyocarditis virus effect [32]. IFN-induced mTOR is LY294002 sensitive and does not affect the IFN-stimulated regulatory element (ISRE) dependent promoter gene activity. A relationship has been observed between the replication of the hepatitis virus and mTOR activity. p21-activated kinase 1 is activated through the mTOR/p70 S6 kinase pathway and regulates the replication of HCV [33]. The IFN induced mTOR activity, independent of PI3K and Akt, is the critical factor for its anti-HCV activity and Jak independent TOR activity involves STAT-1 phosphorylation and nuclear localization, and then PKR is expressed in hepatocytes [31]. No relationship between GGA and mTOR has been reported. However, GGA induced anti-HCV activity depended on mTOR activity independent of PI3-K-Akt, as observed with IFN induced mTOR activity.

When 150 mg of GGA was administered orally, the serum concentration of GGA was approximately 7 μmol/L [34]. The concentration of GGA in the portal blood would be several-fold higher than the serum concentration of GGA; therefore, we speculated that the pharmacological action that would be obtained in clinical practice would be the same as that observed in this study.

GGA, a drug that can be safely administered orally, has mTOR dependent anti-HCV activity. The combination of IFN and GGA has an additive effect on anti-HCV activity. The current results suggest that combination therapy with
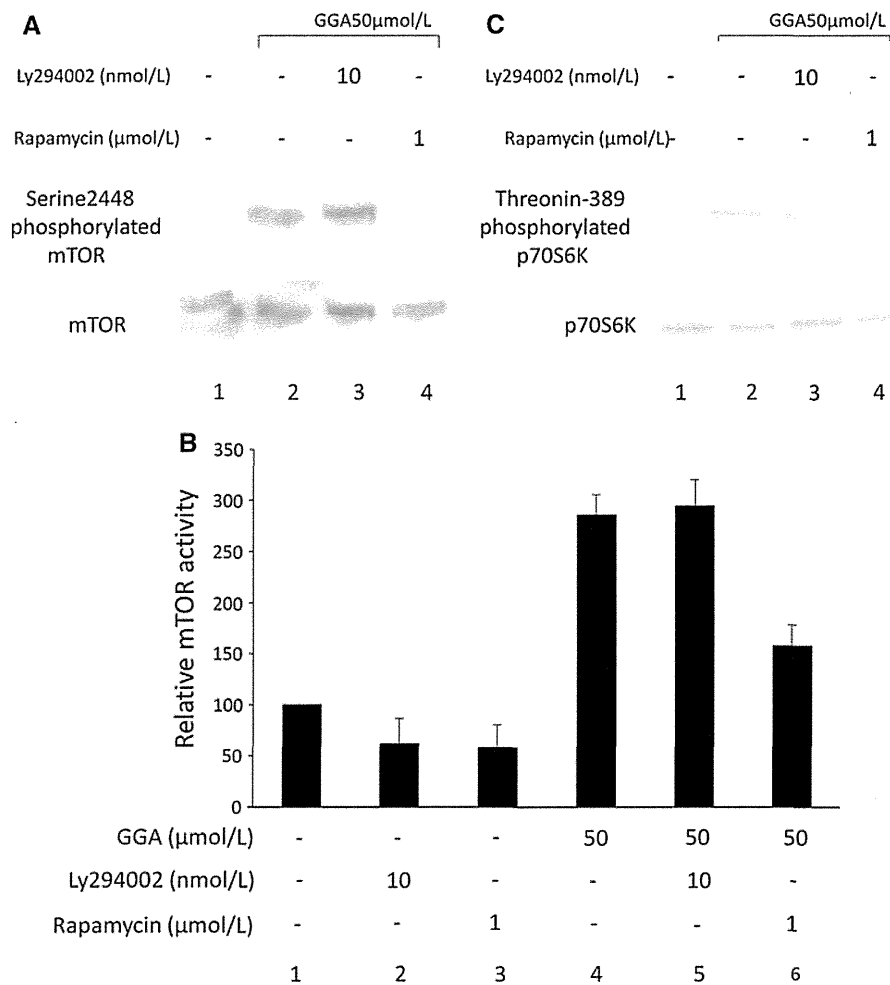
A

		GGA50µmol/L	
Ly294002 (nmol/L)	-	-	10	-
Rapamycin (µmol/L)	-	-	-	1

Serine2448 phosphorylated mTOR

mTOR

1 2 3 4

C

		GGA50µmol/L	
Ly294002 (nmol/L)	-	-	10	-
Rapamycin (µmol/L)	-	-	-	1

Threonin-389 phosphorylated p70S6K

p70S6K

1 2 3 4

B

Relative mTOR activity (350–0)

GGA (µmol/L)	-	-	-	50	50	50
Ly294002 (nmol/L)	-	10	-	-	10	-
Rapamycin (µmol/L)	-	-	1	-	-	1
	1	2	3	4	5	6

Fig. 5 Effect of GGA on mTOR and effect of LY294002 and rapamycin on GGA-induced serine phosphorylated mTOR and threonine phosphorylated p70S6K. **a** After pretreatment with 10 nmol/L LY294002 (*lane 3*) and 1 µmol/L rapamycin (*lane 4*) for 3 h, the OR6 cells were either untreated (*lane 1*) or treated with 50 µmol/L GGA (*lanes 2–4*) for 30 min and then were phosphorylated mTOR at serine-2448 residue (*upper panel*), the expression of mTOR (*lower panel*) was analyzed by Western blotting. **b** After pretreatment with 10 nmol/L LY294002 (*lanes 2 and 5*) and 1 µmol/L rapamycin (*lanes 3 and 6*) for 3 h, the OR6 cells were either untreated (*lanes 1–3*) or treated with 50 µmol/L GGA (*lanes 4–6*) for 30 min.

The mTOR kinase activity was determined by ELISA-based mTOR kinase activity assay kit ($n = 4$). The differences between *lanes 1* and *4*, *lanes 4* and *6*, and *lanes 5* and *6* were statistically significant. The data are expressed as the mean ± SD and are representative of four similar experiments. **c** After pretreatment with 10 nmol/L LY294002 (*lane 3*) and 1 µmol/L, and with rapamycin (*lane 4*) for 3 h, the OR6 cells were either untreated (*lane 1*) or treated with 50 µmol/L GGA (*lanes 2–4*) for 30 min, and then were examined for phosphorylated p70S6K at the threonine-389 residue (*upper panel*), or the expression of p70S6K (*lower panel*) by a Western blotting analysis

GGA and IFN is, therefore, expected to improve the anti-HCV activity. It will, therefore, be necessary to examine the clinical effectiveness of the combination with GGA and IFN for HCV patients in the future.

References

1. Fattovich G, Stroffolini T, Zagni I, Donato F. Hepatocellular carcinoma in cirrhosis: incidence and risk factors. Gastroenterology. 2004;127:S35–50.
2. Pawlotsky JM, Chevaliez S, McHutchison JG. The hepatitis C virus life cycle as a target for new antiviral therapies. Gastroenterology. 2007;132:1979–98.
3. Murakami M, Oketani K, Fujisaki H, Wakabayashi T, Ohgo T. Antiulcer effect of geranylgeranylacetone, a new acyclic polyisoprenoid, on experimentally induced gastric and duodenal ulcers in rats. Arzneimittelforschung. 1981;31:799–804.
4. Murakami M, Oketani K, Fujisaki H, Wakabayashi T, Inai Y, Abe S, et al. Effect of synthetic acyclic polyisoprenoids on the cold-restraint stress induced gastric ulcer in rats. Jpn J Pharmacol. 1983;33:549–56.
5. Hirakawa T, Rokutan K, Nikawa T, Kishi K. Geranylgeranylacetone induces heat shock proteins in cultured guinea pig gastric mucosal cells and rat gastric mucosa. Gastroenterology. 1996;111:345–57.
6. Sakai I, Tanaka T, Osawa S, Hashimoto S, Nakaya K. Geranylgeranylacetone used as an antiulcer agent is a potent inducer of differentiation of various human myeloid leukemia cell lines. Biochem Biophys Res Commun. 1993;191:873–9.

7. Okada S, Yabuki M, Kanno T, Hamazaki K, Yoshioka T, Yasuda T, et al. Geranylgeranylacetone induces apoptosis in HL-60 cells. Cell Struct Funct. 1999;24:161–8.

8. Araki H, Shidoji Y, Yamada Y, Moriwaki H, Muto Y. Retinoid agonist activities of synthetic geranyl geranoic acid derivatives. Biochem Biophys Res Commun. 1995;209:66–72.

9. Kuhen KL, Vessey JW, Samuel CE. Mechanism of interferon action: identification of essential positions within the novel 15-base-pair KCS element required for transcriptional activation of the RNA-dependent protein kinase PKR gene. J Virol. 1998;72:9934–9.

10. Ichikawa T, Nakao K, Nakata K, Hamasaki K, Takeda Y, Kajiya Y, et al. Geranylgeranylacetone induces antiviral gene expression in human hepatoma cells. Biochem Biophys Res Commun. 2001;280:933–9.

11. Ikeda M, Abe K, Dansako H, Nakamura T, Naka K, Kato N. Efficient replication of a full-length hepatitis C virus genome, strain O, in cell culture, and development of a luciferase reporter system. Biochem Biophys Res Commun. 2005;329:1350–9.

12. Tanaka H, Samuel CE. Mechanism of interferon action. Structure of the mouse PKR gene encoding the interferon-inducible RNA-dependent protein kinase. Proc Natl Acad Sci USA. 1994;91:7995–9.

13. Hirakawa T, Rokutan K, Nikawa T, Kishi K. Geranylgeranylacetone induces heat shock proteins in cultured guinea pig gastric mucosal cells and rat gastric mucosa. Gastroenterology. 1996;111:345–57.

14. Uchida S, Fujiki M, Nagai Y, Abe T, Kobayashi H. Geranylgeranylacetone, a noninvasive heat shock protein inducer, induces protein kinase C and leads to neuroprotection against cerebral infarction in rats. Neurosci Lett. 2006;396:220–4.

15. Fujibayashi T, Hashimoto N, Jijiwa M, Hasegawa Y, Kojima T, Ishiguro N. Protective effect of geranylgeranylacetone, an inducer of heat shock protein 70, against drug-induced lung injury/fibrosis in an animal model. BMC Pulm Med. 2009;9:45.

16. Sakabe M, Shiroshita-Takeshita A, Maguy A, Brundel BJ, Fujiki A, Inoue H, et al. Effects of a heat shock protein inducer on the atrial fibrillation substrate caused by acute atrial ischaemia. Cardiovasc Res. 2008;78:63–70.

17. Fudaba Y, Ohdan H, Tashiro H, Ito H, Fukuda Y, Dohi K, et al. Geranylgeranylacetone, a heat shock protein inducer, prevents primary graft nonfunction in rat liver transplantation. Transplantation. 2001;72:184–9.

18. Mochida S, Matsura T, Yamashita A, Horie S, Ohata S, Kusumoto C, et al. Geranylgeranylacetone ameliorates inflammatory response to lipopolysaccharide (LPS) in murine macrophages: inhibition of LPS binding to the cell surface. J Clin Biochem Nutr. 2007;41:115–23.

19. Kanemura H, Kusumoto K, Miyake H, Tashiro S, Rokutan K, Shimada M. Geranylgeranylacetone prevents acute liver damage after massive hepatectomy in rats through suppression of a CXC chemokine GRO1 and induction of heat shock proteins. J Gastrointest Surg. 2009;13:66–73.

20. Hirota K, Nakamura H, Arai T, Ishii H, Bai J, Itoh T, et al. Geranylgeranylacetone enhances expression of thioredoxin and suppresses ethanol-induced cytotoxicity in cultured hepatocytes. Biochem Biophys Res Commun. 2000;275:825–30.

21. Schenk H, Klein M, Erdbrügger W, Dröge W, Schulze-Osthoff K. Distinct effects of thioredoxin and antioxidants on the activation of transcription factors NF-kappa B and AP-1. Proc Natl Acad Sci USA. 1994;91:1672–6.

22. Unoshima M, Iwasaka H, Eto J, Takita-Sonoda Y, Noguchi T, Nishizono A. Antiviral effects of geranylgeranylacetone: enhancement of MxA expression and phosphorylation of PKR during influenza virus infection. Antimicrob Agents Chemother. 2003;47:2914–21.

23. Lin W, Choe WH, Hiasa Y, Kamegaya Y, Blackard JT, Schmidt EV, et al. Hepatitis C virus expression suppresses interferon signaling by degrading STAT1. Gastroenterology. 2005;128:1034–41.

24. Lan KH, Lan KL, Lee WP, Sheu ML, Chen MY, Lee YL, et al. HCV NS5A inhibits interferon-alpha signaling through suppression of STAT1 phosphorylation in hepatocyte-derived cell lines. J Hepatol. 2007;46:759–67.

25. Luquin E, Larrea E, Civeira MP, Prieto J, Aldabe R. HCV structural proteins interfere with interferon-alpha Jak/STAT signalling pathway. Antiviral Res. 2007;76:194–7.

26. Huang Y, Feld JJ, Sapp RK, Nanda S, Lin JH, Blatt LM, et al. Defective hepatic response to interferon and activation of suppressor of cytokine signaling 3 in chronic hepatitis C. Gastroenterology. 2007;132:733–44.

27. Duong FH, Filipowicz M, Tripodi M, La Monica N, Heim MH. Hepatitis C virus inhibits interferon signaling through up-regulation of protein phosphatase 2A. Gastroenterology. 2004;126:263–77.

28. Brender C, Lovato P, Sommer VH, Woetmann A, Mathiesen AM, Geisler C, et al. Constitutive SOCS-3 expression protects T-cell lymphoma against growth inhibition by IFNalpha. Leukemia. 2005;19:209–13.

29. Jia Y, Wei L, Jiang D, Wang J, Cong X, Fei R. Antiviral action of interferon-alpha against hepatitis C virus replicon and its modulation by interferon-gamma and interleukin-8. J Gastroenterol Hepatol. 2007;22:1278–85.

30. Fredericksen B, Akkaraju GR, Foy E, Wang C, Pflugheber J, Chen ZJ, et al. Activation of the interferon-beta promoter during hepatitis C virus RNA replication. Viral Immunol. 2002;15:29–40.

31. Matsumoto A, Ichikawa T, Nakao K, Miyaaki H, Hirano K, Fujimito M, et al. Interferon-alpha-induced mTOR activation is an anti-hepatitis C virus signal via the phosphatidylinositol 3-kinase-Akt-independent pathway. J Gastroenterol. 2009;44:856–63.

32. Kaur S, Lal L, Sassano A, Majchrzak-Kita B, Srikanth M, Baker DP, et al. Regulatory effects of mammalian target of rapamycin activated pathways in type I and II interferon signaling. J Biol Chem. 2007;282:1757–68.

33. Ishida H, Li K, Yi M, Lemon SM. p21-activated kinase 1 is activated through the mammalian target of rapamycin/p70 S6 kinase pathway and regulates the replication of hepatitis C virus in human hepatoma cells. J Biol Chem. 2007;282:11836–48.

34. Hasegawa J, Morishita N, Seki T, Hashida N, Kanazawa T, Sato A. Effect of meals in healthy adult administered Selbex. Syokakika. 1987;7:740–52.

Proteomic Analysis of Hepatitis C Virus (HCV) Core Protein Transfection and Host Regulator PA28γ Knockout in HCV Pathogenesis: A Network-Based Study

Lokesh P. Tripathi,[†,‖] Hiroto Kambara,[‡,‖] Kohji Moriishi,[‡] Eiji Morita,[‡] Takayuki Abe,[‡] Yoshio Mori,[‡] Yi-An Chen,[†,§] Yoshiharu Matsuura,[‡] and Kenji Mizuguchi[*,†,§]
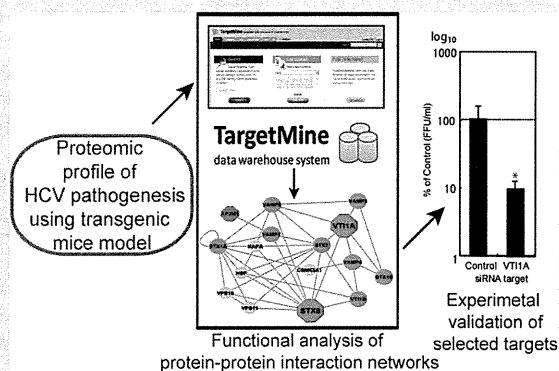
[†]National Institute of Biomedical Innovation, 7-6-8 Saito Asagi, Ibaraki, Osaka, 567-0085, Japan

[‡]Department of Molecular Virology, Research Institute for Microbial Diseases and [§]Graduate School of Frontier Biosciences, Osaka University, 3-1 Yamada-Oka, Suita, Osaka, 565-0871, Japan

Ⓢ Supporting Information

ABSTRACT: Hepatitis C virus (HCV) causes chronic liver disease worldwide. HCV Core protein (Core) forms the viral capsid and is crucial for HCV pathogenesis and HCV-induced hepatocellular carcinoma, through its interaction with the host factor proteasome activator PA28γ. Here, using BD-PowerBlot high-throughput Western array, we attempt to further investigate HCV pathogenesis by comparing the protein levels in liver samples from Core-transgenic mice with or without the knockout of PA28γ expression (abbreviated PA28γ^{−/−}CoreTG and CoreTG, respectively) against the wild-type (WT). The differentially expressed proteins integrated into the human interactome were shown to participate in compact and well-connected cellular networks. Functional analysis of the interaction networks using a newly developed data warehouse system highlighted cellular pathways associated with vesicular transport, immune system, cellular adhesion, and cell growth and death among others that were prominently influenced by Core and PA28γ in HCV infection. Follow-up assays with *in vitro* HCV cell culture systems validated VTI1A, a vesicular transport associated factor, which was upregulated in CoreTG but not in PA28γ^{−/−}CoreTG, as a novel regulator of HCV release but not replication. Our analysis provided novel insights into the Core-PA28γ interplay in HCV pathogenesis and identified potential targets for better anti-HCV therapy and potentially novel biomarkers of HCV infection.

Functional analysis of protein-protein interaction networks

Experimetal validation of selected targets

KEYWORDS: CoreTG, GO, HCC, HCV, KEGG, OMIM, PA28γ^{−/−}CoreTG, PPI, siRNA, TargetMine

◼ INTRODUCTION

Hepatitis C virus (HCV) is a prime cause of chronic liver disease frequently characterized by liver inflammation with accompanying steatosis, progressive fibrosis, and hepatocellular carcinoma (HCC) and infects nearly 3% of the world's population. HCV contains a single-stranded RNA genome encoding a 3000-amino-acid polyprotein, which is processed by host and viral factors to yield 10 viral proteins, Core, E1, E2, p7, NS2, NS3, NS4A, NS4B, NS5A, and NS5B.[1−4] HCV variants are classified into six major genotypes with multiple subtypes characterized by phylogenetic heterogeneity, differences in infectivity, and interferon sensitivity.[5,6] The availability of cell-culture-based systems for HCV infection has provided an increased understanding of HCV pathogenesis.[5,7−9] Transgenic mice (preferably C57BL strain) expressing HCV proteins in the liver are also a preferred choice for the investigation of HCV pathogenesis.[10] However, despite considerable research efforts, precise molecular mechanisms underlying HCV pathology remain unclear.

HCV Core protein (hereafter referred to as Core) is spliced from the polyprotein by the signal peptidase and further processed into a highly conserved 21-kDa mature form by the signal peptide peptidase; this processing facilitates its transfer to the detergent-resistant membrane fraction where virus replication and assembly take place. Core is a multifunctional protein implicated in RNA binding and as a pathogenic factor; it induces steatosis and HCC and, thus, liver failure.[1,10] The ubiquitin-proteasome pathway, the premier intracellular protein degradation system in eukaryotes, is a key regulator of cellular processes and is also associated with the evasion of host immune response by many viruses, viral maturation, and progeny release.[11] Core binds to the proteasome activator PA28γ in the nucleus and is degraded via a PA28γ-dependent pathway. PA28γ plays a crucial role in Core-induced insulin resistance, steatogenesis, and hepatocarcinogenesis and in HCV propagation; PA28γ knockout in Core transgenic mice disrupts

steatosis and HCC, restores insulin sensitivity, and impairs viral particle production, and thus PA28γ is a promising target for anti-HCV therapies with minimal side effects.[2,12-13] However, the exact mechanisms through which PA28γ facilitates Core-induced HCV pathogenesis remain poorly understood.

In this study, we aim to put forth biological networks that describe the differential expression of the host proteins and their likely roles in modulating PA28γ function in HCV pathogenesis. We employed PowerBlot Western Array screening system, a high-throughput Western blotting method, to identify changes at the proteome level in Core expressing transgenic C57BL/6 mice with or without the knockout of PA28γ gene expression (abbreviated PA28$\gamma^{-/-}$CoreTG and CoreTG, respectively). In our analysis, we included human protein interaction data and gene regulatory information for the differentially expressed proteins using TargetMine, an integrated data warehouse that we have developed recently.[16] Our network-based analyses of the proteomic changes from the three data sets (CoreTGvsC57BL/6, PA28$\gamma^{-/-}$Core-TGvsC57BL/6 and PA28$\gamma^{-/-}$CoreTGvsCoreTG) provided novel insights into PA28γ function in Core-induced HCV pathogenesis. Furthermore, we identified VTI1A, a vesicular transport associated factor, which was upregulated in CoreTG but not in PA28$\gamma^{-/-}$CoreTG, as a novel regulator of HCV release and, thus, an attractive target for anti-HCV therapy.

■ MATERIALS AND METHODS

Protein Sample Preparation

Protein samples were prepared from the livers of the C57BL/6 wild-type (hereafter referred to as WT) and the transgenic mice expressing HCV Core protein genotype 1b line C49 with (PA28$\gamma^{-/-}$CoreTG) or without (CoreTG) the knockout of PA28γ expression.[2,12] Livers were harvested from three individuals each of WT, CoreTG, and PA28$\gamma^{-/-}$CoreTG mice, and the harvested samples for each mice type were pooled together prior to protein sample preparation for PowerBlot analysis. The pooled liver samples of each mice type were homogenized in 1x sample buffer of SDS-PAGE on ice and then boiled for 5 min. The boiled sample was sonicated for the viscosity of DNA and employed for PowerBlot analysis.

PowerBlot Western Array Analysis

The levels of differentially expressed proteins were determined by the PowerBlot assay by BD Biosciences Pharmingen (San Diego, CA, USA). Briefly, samples containing 200 μg of protein was loaded in one big well on top of a 4–15% gradient SDS-polyacrylamide gel and separated by electrophoresis (1.5 h at 150v). The proteins were transferred to Immobilon-FL membrane (Millipore, Billerica, MA, USA) for 2 h at 200 mA. After transfer, the membranes were incubated in the blocking buffer (LI-COR, Lincoln, NE, USA). The membrane was clamped with a Western blotting manifold that isolates 41 channels across the membrane. Each channel was incubated with a complex antibody cocktail for 1 h. The blots were removed from the manifold, washed, and hybridized for 30 min with secondary goat anti-mouse antibody conjugated to Alexa680 fluorescent dye (Molecular Probes, Eugene, OR, USA). Image data were captured using the Odyssey Infrared Imaging System (LI-COR). Data analysis included the raw and normalized signal intensity data from each blot. The results were expressed as fold change that represented the protein changes, either increasing or decreasing in the comparative analysis between the experimental samples and the control.

The detected protein expression changes were listed in the order of confidence, 0 through 3, with 3 being the highest level of confidence, based on the signal quality. Only the data from confidence levels 2 and 3 (good quality signals; Supporting Information; Tables S1, S2a, S2b, and S2c) for proteins mapped to valid accessions were considered for further analysis. Proteins that displayed >1.8-fold change in abundance were judged to be differentially expressed, following the manufacturer's recommendation.

Human Orthologues for the Differentially Expressed Proteins

BD PowerBlot assay employs a cocktail of monoclonal antibodies that target human, mouse, and rat proteins, and in a specific study, over 90% were found to cross-react with proteins from human, mouse and rat[17] (Table S1). Human orthologues for the proteins picked up by the antibody cocktail were retrieved from KEGG (Tables S2a, S2b, and S2c).

Construction of Protein–Protein Interaction Networks

PPIs for the human orthologues of each set of differentially expressed proteins were retrieved from BioGRID 3.1.74[18] and iRefIndex 8.0[19] databases along with the interactions between the primary interactors of the differentially expressed proteins using TargetMine.[16] TargetMine is an integrated data warehouse that combines different biological data types and employs an objective protocol to prioritize candidate genes for further experimental investigation.[16] The interactions were merged and filtered for redundancy to infer overall extended PPI networks. Protein identifiers used in the different databases were mapped to Entrez gene IDs and official gene symbols. The official gene symbols are used hereafter, to refer to the differentially expressed proteins (Table 1) and their interacting partners. All the relationships discussed should be interpreted as protein relationships unless otherwise clarified.

PPI Network Topological Analysis

Network components were visualized using Cytoscape 2.6,[20] while network properties such as node degree distribution and shortest path measures were computed using the Cytoscape NetworkAnalyzer plugin[21] as described previously.[22] In a PPI network, the degree of a node (protein) is defined as the number of nodes directly connected to (interacting with) it, i.e., its first neighbors. Node degree distribution, $P(k)$, is the number of nodes with a degree k for k = 0, 1, 2, ... The shortest path length between two nodes n and m, $L(n,m)$, is the minimal number of interactions that link proteins n and m in a PPI network. The shortest path length distribution is the number of node pairs (n,m) with $L(n,m) = x$ for x = 1, 2, ... The average shortest path length, also known as the characteristic path length, gives the expected distance between two connected nodes i.e. the minimal number of interactions that link any two proteins in a PPI network.

Functional Analysis by Characterization of Enriched Biological Associations

Gene ontology (GO) associations retrieved from GO consortium,[23] biological pathway data from KEGG (retrieved on March 1, 2011),[24] and disease phenotype associations from OMIM[25] were used to assign functional annotations to the constituents of the extended PPI networks. The proteins in each of the extended PPI networks were uploaded to TargetMine to create protein lists, and the enrichment of specific biological themes (GO terms, KEGG Pathways, OMIM phenotypes) associated with each PPI network was estimated

Table 1. Summary of PowerBlot Detected Protein Expression Levels in Protein Samples

CoreTGvsWT

protein	gene ID	symbol	confidence level[a]	(−) under, (+) over[b]	fold change[c]
P31749	207	AKT1	3	−	2.68
P07355	302	ANXA2	3	+	2.92
O43747	164	AP1G1	3	+	5.72
P63010	163	AP2B1	3	+	2.40
Q96CW1	1173	AP2M1	2	+	1.93
Q9Y2T2	26985	AP3M1	2	+	1.89
P05089	383	ARG1	2	+	2.08
P52566	397	ARHGDIB	3	+	2.02
O15145	10094	ARPC3	2	−	2.25
P49407	408	ARRB1	3	−	2.33
Q07812	581	BAX	3	+	2.03
P55212	839	CASP6	3	−	1.95
Q14790	841	CASP8	2	+	2.18
Q03135	857	CAV1	2	+	2.07
P12830	999	CDH1	3	−	2.33
P19022	1000	CDH2	3	+	4.57
Q53SH4	1134	CHRNA1	3	−	3.11
P21964	1312	COMT	2	+	2.96
P00450	1356	CP	3	+	2.36
P21291	1465	CSRP1	3	+	2.23
P49711	10664	CTCF	3	+	6.13
P25685	3337	DNAJB1	3	−	2.16
P63241	1984	EIF5A	3	+	1.94
P42566	2060	EPS15	3	+	4.28
Q92889	2072	ERCC4	3	+	5.43
O75899	9568	GABBR2	3	+	3.39
O43719	27336	HTATSF1	3	+	5.76
P06756	3685	ITGAV	3	+	6.32
Q14974	3837	KPNB1	3	−	1.86
Q16539	1432	MAPK14	3	−	2.81
Q9UPY8	22924	MAPRE3	3	+	2.46
P49736	4171	MCM2	3	+	1.87
P62166	23413	NCS1	3	−	2.24
Q8IZ57	140767	NRSN1	3	+	1.89
Q16620	4915	NTRK2	3	+	2.40
Q14980	4926	NUMA1	3	−	1.94
P07237	5034	P4HB	3	+	2.27
Q92878	10111	RAD50	3	+	4.93
Q99638	5883	RAD9A	2	−	3.10
P20936	5921	RASA1	3	+	1.86
Q96SB4	6732	SRPK1	3	+	3.11
Q92186	8128	ST8SIA2	3	+	5.11
P42224	6772	STAT1	3	+	2.00
P40763	6774	STAT3	3	+	2.30
Q9UNK0	9482	STX8	3	+	1.88
Q12800	7024	TFCP2	3	+	5.04
Q92752	7143	TNR	3	+	5.36
Q13263	10155	TRIM28	3	+	4.70
O43396	9352	TXNL1	3	−	4.82
P50552	7408	VASP	2	−	2.61
Q96AJ9	143187	VTI1A	3	+	3.25
Q14191	7486	WRN	3	+	17.12

altered protein levels in PA28γ−/−CoreTGvsWT

protein	gene ID	symbol	confidence level[a]	(−) under, (+) over[b]	fold change[c]
O15145	10094	ARPC3	2	−	1.96
P49407	408	ARRB1	3	−	2.17
P55212	839	CASP6	3	−	2.04
O60508	51362	CDC40	2	+	1.99
P54105	1207	CLNS1A	3	+	2.41
P21964	1312	COMT	2	+	2.71
P67870	1460	CSNK2B	3	+	1.90
P78352	1742	DLG4	2	+	4.08
Q95GK7	1837	DTNA	3	−	2.42
P55010	1983	EIF5	3	+	2.19
Q08495	2039	EPB49	3	+	2.66
P37268	2222	FDFT1	2	+	5.68
P09038	2247	FGF2	2	+	2.69
P62962	2280	FKBP1A	2	+	1.89
O75146	9026	HIP1R	2	−	2.08
Q9NZL4	23640	HSPBP1	3	+	3.46
P05412	3725	JUN	2	+	2.15
P52292	3838	KPNA2	3	−	7.28
P36507	5605	MAP2K2	3	−	2.35
Q16539	1432	MAPK14	3	−	3.29
P22033	4594	MUT	3	+	2.46
P54920	8775	NAPA	2	−	1.97
Q8IZ57	140767	NRSN1	3	+	1.93
Q16620	4915	NTRK2	3	+	2.50
P07237	5034	P4HB	3	+	2.04
Q08209	5530	PPP3CA	3	+	7.55
Q06124	5781	PTPN11	2	+	2.33
Q99638	5883	RAD9A	2	−	1.97
P43487	5902	RANBP1	3	+	2.29
Q9UPX8	22941	SHANK2	3	−	1.94
P29353	6464	SHC1	3	+	3.27
Q92186	8128	ST8SIA2	3	+	4.06
P31948	10963	STIP1	3	−	1.99
O75558	8676	STX11	2	+	2.04
P23193	6917	TCEA1	3	−	2.17
P07101	7054	TH	2	+	2.78
P13693	7178	TPT1	3	−	1.93
Q15628	8717	TRADD	3	−	2.00
P50607	7275	TUB	3	+	1.91

altered protein levels in PA28γ−/−CoreTGvsCoreTG

protein	gene ID	symbol	confidence level[a]	(−) under, (+) over[b]	fold change[c]
P07355	302	ANXA2	3	−	2.96
O43747	164	AP1G1	3	−	4.20
P63010	163	AP2B1	3	−	3.01
Q96CW1	1173	AP2M1	2	−	1.88
Q9Y2T2	26985	AP3M1	3	+	2.38
O00499	274	BIN1	2	−	1.88
Q9UQM7	815	CAM2KA	3	+	2.06
Q8N5S9	84254	CAMKK1	2	+	5.78
P19022	1000	CDH2	3	−	3.85
P25108	1134	CHRNA1	3	+	2.55
P49674	1454	CSNK1E	3	+	1.97
P67870	1460	CSNK2B	3	+	1.88
P21291	1465	CSRP1	3	+	1.87
P49711	10664	CTCF	3	−	5.43
Q8WTW3	9382	COG1	3	−	7.02
P00450	1356	CP	3	−	3.55
Q13618	8452	CUL3	3	+	1.91
P78352	1742	DLG4	2	+	2.13
Q9Y4J8	1837	DTNA	3	−	2.94

Table 1. continued

altered protein levels in PA28γ−/−CoreTGvsCoreTG					
protein	gene ID	symbol	confidence level[a]	(−) under, (+) over[b]	fold change[c]
Q08495	2039	EBP49	3	+	2.30
O14682	8507	ENC1	3	+	2.88
P42566	2060	EPS15	3	−	2.11
Q92889	2072	ERCC4	3	−	3.49
P09038	2247	FGF2	2	−	2.18
P62962	2280	FKBP1A	2	+	2.59
P49356	2342	FNTB	2	+	1.95
O75899	9568	GABBR2	3	−	2.53
O75146	9026	HIP1R	3	−	1.97
Q9NZL4	23640	HSPBP1	3	+	3.60
P61604	3336	HSPE1	3	−	2.17
Q99730	27336	HTATSF1	3	−	9.24
Q9Y6K9	8517	IKBKG	2	+	1.97
P52292	3838	KPNA2	3	−	3.94
P36507	5605	MAP2K2	3	−	2.66
Q13505	4580	MTX1	3	−	1.90
P62166	23413	NCS1	3	+	2.56
Q14980	4926	NUMA1	2	+	1.87
P41236	5504	PPP1R2	3	−	2.25
Q08209	5530	PPP3CA	3	+	12.94
P13861	5576	PRKAR2A	3	−	1.88
Q15276	9135	RABEP1	2	−	2.74

altered protein levels in PA28γ−/−CoreTGvsCoreTG					
protein	gene ID	symbol	confidence level[a]	(−) under, (+) over[b]	fold change[c]
Q92878	10111	RAD50	3	−	5.19
P20936	5921	RASA1	3	+	2.50
P06400	5925	RB1	3	+	2.50
Q92854	10507	SEMA4D	2	+	2.00
Q92529	53358	SHC3	3	−	1.90
P63208	6500	SKP1	3	−	2.45
P43004	6506	SLC1A2	2	+	2.27
Q4U2R8	9356	SLC22A6	3	−	2.23
P42224	6772	STAT1	3	−	1.90
P31948	10963	STIP1	3	−	1.98
O75558	8676	STX11	2	+	3.52
Q8IZU3	50511	SYCP3	3	+	1.88
P07101	7054	TH	2	+	2.62
Q92752	7143	TNR	3	−	4.62
O43396	9352	TXNL1	2	+	3.05
P13693	7178	TPT1	3	−	2.85
Q13263	10155	TRIM28	3	−	3.53
Q15628	8717	TRADD	3	−	2.98
P50607	7275	TUB	3	+	1.96
P41542	8615	USO1	3	−	2.05
Q14191	7486	WRN	3	−	3.44

[a]Defined as follows: Level 3 = changes greater than 2-fold from good quality signals that also pass a visual inspection. Level 2 = changes greater than 2-fold from good quality signals that do not pass a visual inspection. [b]+ indicates an increase in protein level in the experimental sample relative to control. − indicates a decrease in protein level in the experimental sample relative to control. [c]A semiquantitative value that represents the general trend of protein changes for the experimental sample relative to control.

by performing the hypergeometric test within TargetMine.[16] The inferred p-values were further adjusted for multiple test correction to control the false discovery rate using the Benjamini and Hochberg procedure,[26,27] and the annotations/pathways were considered significant if $p \leq 0.05$.

Transcription Factor-Target Associations

Transcription factor (TF)-target associations for the differentially expressed proteins were retrieved from the TF-target repository compiled from Amadeus[28] and ORegAnno[29] in TargetMine[16] and are discussed in the Supporting Information.

RNAi and Transfection

The siRNA pair targets to VTI1A, STX8, and COMT were purchased from Ambion (Ambion, Austin, TX, USA). Stealth RNAi Negative Control Low GC Duplex (Invitrogen, Carlsbad, CA, USA) was used as a control siRNA. Each siRNA duplex was introduced into the cell lines by using lipofectamine RNAiMax (Invitrogen). Ambion ID numbers of siRNA duplex of VTI1A and STX8 were S225671 and S18183, respectively. The replicon cell line, as will be described below, was transfected with each siRNA at a final concentration of 20 nM as per the manufacturer's protocol and then seeded at 2.5 × 10⁴ cells per well of a 24-well plate. The transfected cells were harvested at 72 h post-transfection. The Huh7OK1 cell line, as will be described below, was transfected with each siRNA at a final concentration of 20 nM as per the manufacturer's protocol and then seeded at 2.5 × 10⁴ cells per well of a 24-well plate. The transfected cells were infected with JFH1 at an MOI of 0.05 at 24 h post-transfection. The resulting cells were harvested at the indicated time.

Quantitative Reverse-Transcription PCR (qRT-PCR)

Total RNA was prepared from the cell and culture supernatant using the RNeasy mini kit (QIAGEN, Hilden, Germany) and QIAamp Viral RNA Mini Kit (QIAGEN), respectively. First-strand cDNA was synthesized using a high capacity cDNA reverse transcription kit (Applied Biosystems, Carlsbad, CA, USA) with random primers. Each cDNA was estimated by Platinum SYBR Green qPCR Super Mix UDG (Invitrogen) as per the manufacturer's protocol. Fluorescent signals of SYBR Green were analyzed with ABI PRISM 7000 (Applied Biosystems). The HCV internal ribosomal entry site (IRES) region and human glyceraldehyde-3-phosphate dehydrogenase (GAPDH) gene were amplified with the primer pairs 5′-GAGTGTCGTGCAGCCTCCA-3′ and 5′-CACTCGCAAG-CACCCTATCA-3′, and 5′-GAAGGTCGGAGTCAACG-GATT-3′ and 5′-TGATGACAAGCTTCCCGTTCTC-3′, respectively.[30] The quantities of the HCV genome and the other host mRNAs were normalized with that of GAPDH mRNA. VTI1A and STX8 genes were amplified using the primer pairs 5′-TGACAGGGATGTTGCGAAGA-3′ and 5′-CAACCCACATGCAAACAGGA-3′, and 5′-TTGAAGGG-GACCGAAGACAGAACCTC-3′, and 5′-TCAAAACCCAA-GCCTCTGGTCTCCT-3′, respectively.

Cell Lines and Virus Infection

Cells from the Huh7OK1 cell line are highly permissive to HCV JFH1 strain (genotype 2a) infection compared to Huh 7.5.1 and exhibit the highest propagation efficiency for JFH1.[30] These cells were maintained at 37 °C in a humidified atmosphere and 5% CO_2, in Dulbecco's modified Eagle's medium (DMEM) (Sigma, St. Louis, MO, USA) supplemented with nonessential amino acids (NEAA), sodium pyruvate, and

10% fetal calf serum (FCS). The human hepatoma cell line Huh7, harboring the full genome of the HCV Con1 strain (genotype 1b), was prepared as described by Pietschmann et al.[31] We also established an Huh7 cell line harboring the subgenome of the JFH1 strain by the transfection of the plasmid pSGR-JFH1.[32] The Huh7-derived cell lines harboring a full length HCV replicon were maintained in DMEM containing 10% FCS, nonessential amino acids, sodium pyruvate, and 1 mg/mL G418 (Nakarai Tesque, Tokyo, Japan). The viral RNA of JFH1 was introduced into Huh7OK1 as described by Wakita et al.[33] The viral RNA of JFH1 derived from the plasmid pJFH1 was prepared as described by Wakita et al.[33]

Statistical Analysis

Experiments for RNAi transfection and qRT-PCR were performed three times. The estimated values were represented as the mean $\pm$ standard deviation ($n = 3$). The significance of differences in the means was determined by the Student's t test.

RESULTS AND DISCUSSION

Core Expression and PA28γ Knockout Induce Substantial Changes in the Expression Levels of Host Proteins Associated with HCV Infection in the Liver

The PowerBlot immunoblots showed proteins with increased or decreased levels (defined as those that displayed >1.8-fold change in abundance) in the transgenic samples relative to the WT samples and also relative to each other. In all, we identified 37 proteins with increased levels and 15 proteins with decreased levels in CoreTGvsWT, 24 proteins with increased levels and 15 proteins with decreased levels in PA28γ$^{-/-}$-CoreTGvsWT, and 26 proteins with increased levels and 36 proteins with decreased levels in PA28γ$^{-/-}$CoreTGvsCoreTG. While most proteins with altered abundance display changes between 1.8-fold and 6-fold, some proteins displayed much higher fold changes. For instance, WRN protein levels increased 17-fold in CoreTGvsWT (Table 1).

Our analysis detected changes in the abundance of proteins, known to be associated with HCV pathogenesis, in the liver samples from CoreTG compared with WT. These include Arginase I (ARG1; +2.08-fold), a liver enzyme associated with the polyamine metabolism, which is known to be overexpressed in HCV-mediated hepatocarcinogenesis;[34] STAT3 (+2.30-fold), which is directly activated by the Core and HCV-mediated oxidative stress facilitating tumorigenesis and is also essential for HCV replication;[35−37] STAT1 (+2-fold), which interacts with Core and facilitates the HCV-mediated attenuation of the host interferon signaling;[38] and MAPK14 (p38 MAPK; −2.81-fold), which is cooperatively activated by Core and ethanol in HCV infection[39] (Table 1). These results are in line with the previous observations that Core expression can induce HCV pathogenesis and hepatocarcinogenesis in transgenic mice.[2] Among other examples, BIN1, which interacts with the HCV NS5A protein and contributes to the pathogenesis of HCC,[40] was suppressed 1.88-fold in PA28γ$^{-/-}$CoreTGvsCoreTG; this is consistent with the lack of HCC pathogenesis in PA28γ$^{-/-}$CoreTG mice. Similar studies have aimed to characterize the global changes in the host transcriptome and proteome in response to HCV infection.[41−44] These studies, however, have not provided specific insights into PA28γ's roles in HCV pathogenesis. Our observations suggest that the PowerBlot assay was able to capture successfully some of the molecular signatures associated with the Core-PA28γ interplay in HCV pathogenesis.

Topological Analysis of the Extended Protein Interaction Networks

To further understand the biological significance of the differential protein levels, we retrieved PPIs for the proteins with increased and decreased levels in CoreTGvsWT, PA28γ$^{-/-}$CoreTGvsWT, and PA28γ$^{-/-}$CoreTGvsCoreTG and inferred the corresponding extended protein interaction networks for each data set using TargetMine (see Materials and Methods). First, we computed the *node degree distribution* and *characteristic/average path length* measures to capture the topology of the extended PPI networks as described earlier.[22] The degree of a protein, which corresponds to the number of its interacting partners, may often reflect its biological relevance since a better connected protein may have a higher ability of influencing biological networks via PPIs. Average path lengths provide an approximate measure of the relative ease and speed of transfer of information between the proteins in a network. The CoreTGvsWT extended network was made up of 1373 entities (proteins) with 12535 interactions, the PA28γ$^{-/-}$CoreTGvsWT extended network of 1057 entities with 8988 interactions, and the PA28γ$^{-/-}$CoreTGvsCoreTG of 1476 entities with 12871 interactions between them, respectively (Tables S3, S4). For comparison, we also derived an extended PPI network for all the non-genetic PPIs in the human genome as compiled in BioGRID and iRefindex repositories (data not shown). The average degree (defined as the number of interactions for a given protein) of the CoreTGvsWT (17.31), PA28γ$^{-/-}$CoreTGvsWT (16.1), and PA28γ$^{-/-}$CoreTGvsCoreTG (16.57) extended networks was higher than the degree inferred for the human interactome (10.17). This observation suggests that HCV infection targets several highly connected cellular proteins with an ability to influence a large number of host factors in HCV pathogenesis. The average (shortest) path lengths of the three extended networks (2.93, 2.9, and 2.97, respectively) were significantly shorter than that inferred for the human interactome (3.88), suggesting that the Core and PA28γ influenced cellular networks are more compact and inclined toward faster communication between the constituents relative to the human interactome (Figure 1). Our observations are consistent with previous studies on the protein interaction networks associated with HCV infection.[22,45]

The compactness of the HCV-influenced protein networks coupled with the ability to influence a wide array of factors in the host cellular networks may facilitate a rapid propagation of the signaling information and allow the virus to respond rapidly to the host mobilization against HCV infection.

Functional Analysis of the Extended Protein Interaction Networks

Next, we investigated the extended networks for the enrichment of specific biological associations (KEGG pathways, GO terms, and OMIM phenotypes, Tables S5, S6, and S7). The analysis of the CoreTGvsWT, PA28γ$^{-/-}$CoreTGvsWT, and PA28γ$^{-/-}$CoreTGvsCoreTG extended networks revealed an enrichment ($p \leq 0.05$) of 116, 104, and 118 KEGG pathways, respectively (Table S5). Below we describe our observations on the selected enriched biological themes of interest, chiefly associated with the PA28γ$^{-/-}$CoreTGvsCoreTG network. Functional associations for the host factors previously known to be associated with HCV pathogenesis and HCC are
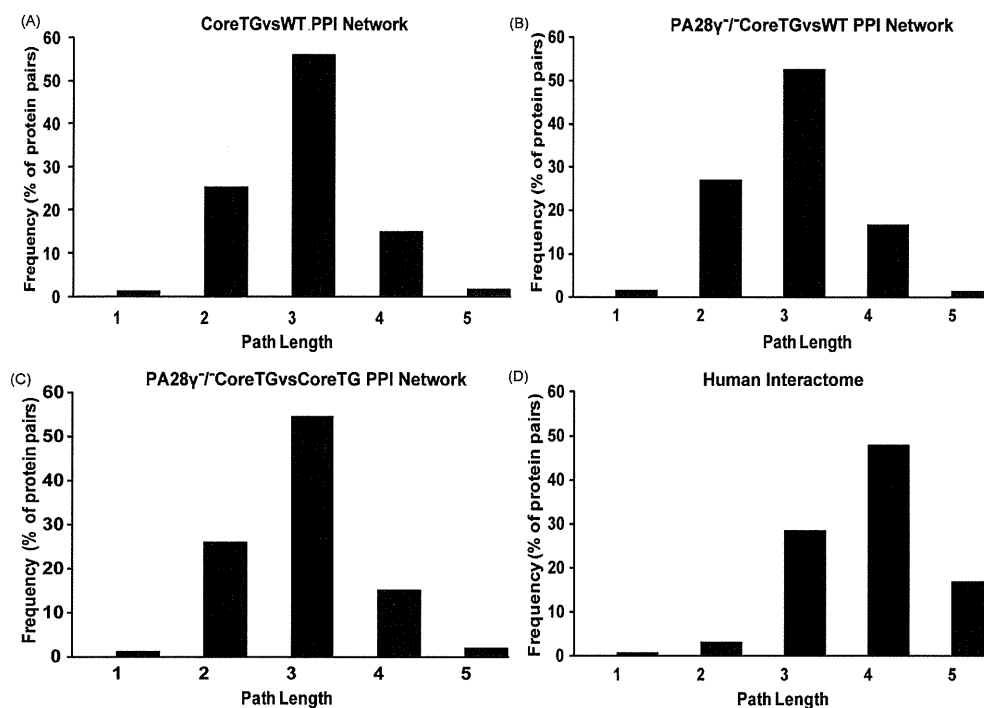
Figure 1. Graphical representation of the shortest path length distribution for (A) CoreTGvsWT extended network, (B) PA28γ$^{-/-}$CoreTGvsWT extended network, (C) PA28γ$^{-/-}$CoreTGvsCoreTG extended network, and (D) human protein interactome. The path length is represented on the x-axis, while the y-axis describes the frequency, i.e., the percentage of node (protein) pairs within the PPI network with a given shortest path length. For simplicity, only the node frequencies for path lengths 1—5 are displayed.

summarized in Table 2. Specific functional associations for the CoreTGvsWT and PA28γ$^{-/-}$CoreTGvsWT networks, except when discussed below, are detailed in the Supporting Information. It will highlight the biological significance of the differentially expressed proteins, their interactions, and their probable roles in HCV infection and help identify potentially novel regulators of and biomarkers for HCV pathogenesis.

Vesicular Transport

HCV infection involves the formation of the HCV replication complex in the detergent-resistant membrane (DRM) fraction or lipid rafts. These subcellular membrane fractions are utilized by some pathogens including viruses to facilitate viral entry and assembly.[46−49] HCV infection induces modifications in the host lipid raft proteome, which directly impacts HCV replication in the infected cells.[50] Core targeting to the early and late endosomes and the viral particle production requires the components of the endosome-based secretory pathways.[51,52]

CoreTGvsWT Extended Network. The PowerBlot analysis revealed the two endosomal proteins VTI1A and STX8 (KEGG Pathway "SNARE interactions in vesicular transport"; p = 0.023; Table S5) that were upregulated 3.25- and 1.88-fold, respectively, in CoreTGvsWT (Table 1). SNAREs are membrane-anchored proteins involved in membrane trafficking.[53] Some SNAREs may function in HCV egress by possibly facilitating the fusion of the late endosomes that carry HCV particles with the plasma membrane resulting in their release into the extracellular environment.[52] VTI1A is a SNARE involved in the vesicular transport from the late endosomes to the trans-Golgi network and forms a SNARE complex with STX16 and VAMP4 (Table S4).[54,55] STX8 is involved in the protein trafficking from the early to the late endosomes and exocytosis and forms a SNARE complex with STX7, VAMP8,

and VTI1B.[55,56] A reduction in the expression of STX7, which interacts with both VTI1A and STX8 (Figure 2; Table S4), decreases HCV replication.[50] Taken together, the increased abundances of VTI1A and STX8 in CoreTGvsWT, but not PA28γ$^{-/-}$CoreTGvsWT, suggest potentially crucial roles of the two proteins in the HCV life cycle.

PA28γ$^{-/-}$CoreTGvsCoreTG Extended Network. Syntaxin 11 (STX11), a SNARE, was upregulated 3.52-fold in PA28γ$^{-/-}$CoreTGvsCoreTG (Table 1) and was mapped to the enriched KEGG Pathway "SNARE interactions in vesicular transport" (p = 0.003; Table S5). STX11 associates with the late endosomes and functions in the essential trafficking pathways (such as cytokine secretion) in the immune cells, with enhanced STX11 expression contributing to increased NK-cell mediated cytotoxicity.[57−61] STX11 binds with the SNARE VTI1B (Figure 3, Table S4) and regulates its participation the Q-SNARE complexes and, thus, the endocytic and exocytic trafficking in the macrophages. Overexpression of STX11 alters the VTI1B binding to STX6 and STX8 and likely reduces the endosomal transport to the cell surface.[57]

USO1, a Golgi-associated peripheral membrane protein, was decreased 2.05-fold in PA28γ$^{-/-}$CoreTGvsCoreTG (Table 1) and was identified as a significant linking component of the PA28γ$^{-/-}$CoreTGvsCoreTG SNARE network (Figure 3). USO1 plays an important role in ER to Golgi trafficking and its knockdown leads to the disintegration of the Golgi complex.[62,63] Decreased USO1 levels in PA28γ$^{-/-}$CoreTGvsCoreTG may, therefore, significantly impact the endosomal pathways associated with HCV release.

PA28γ knockdown impairs the production of the infectious HCV particles (but not replication) in the JFH1 (HCV genotype 2a) infected cells, largely due to the deregulation of the E6AP-dependent Core degradation, which contributes to an antiviral response.[14] Our analysis suggests a potentially novel

Table 2. Functional Analysis of the Extended Protein Interaction Networks[a]

proteins	data set[b]	KEGG pathways	prior involvement with HCV pathogenesis and HCC	probable associations with Core/PA28γ functions in HCV pathogenesis
AKT1	I (−)	Insulin signaling pathway ($p = 5.72 \times 10^{-12}$)	reduced levels associated with insulin resistance (IR) in rats;[105] Akt phosphorylation is suppressed in the CoreTG mice and contributes to IR.[12]	Core-induced suppression of AKT1 levels may contribute to IR in HCV pathogenesis.
BAX	I (+)	Apoptosis ($p = 1.58 \times 10^{-18}$)	interacts with NS5A; disrupts mitochondrial homeostasis leading to abnormal cytochrome c release and apoptosis in HCV infection.[45,90,92,93]	Core-mediated BAX upregulation may induce host cell apoptosis.
CASP8	I (+)	Apoptosis ($p = 1.58 \times 10^{-18}$)	activated in HCV infection.[90]	Core-mediated CASP8 upregulation may induce host cell apoptosis.
CDH1	I (+)	Adherens junction ($p = 1.45 \times 10^{-20}$)	downregulated in the rat liver during hepatocarcinogenesis[106]	Core-mediated decrease in CDH1 levels may contribute to HCC
COMT	I (+); II (+)	Steroid hormone biosynthesis ($p = 0.002$)	upregulated in the lipid rafts in HCV infection;[50] COMT siRNA knockdown decreases HCV replication[103]	Core-induced activation of COMT may play an important role in HCV entry and replication
CSNK2B	II (+); III (+)	Adherens junction ($p = 1.4 \times 10^{-13}$); tight junction ($p = 4.46 \times 10^{-7}$)	interacts with the HCV NS3 protein;[45] regulates NS5A phosphorylation and hence infectious HCV particle production.[87]	loss of PA28γ activity may perturb CK2-mediated NS5A phosphorylation leading to decreased viral propagation.
EPS15	I (+); III (−)	Endocytosis ($p = 2.08 \times 10^{-22}$)	elevated in human and mouse HCC;[107] mediates human enterovirus 71 entry via clathrin-mediated endocytosis,[108] which also mediates HCV internalization.[109]	elevated EPS15 levels may facilitate HCC; decreased EPS15 levels may contribute to the lack of HCC in the PA28γ−/−CoreTG. May facilitate HCV entry via clathrin-mediated endocytosis.
MCM2	I (+)	Cell cycle ($p = 1.82 \times 10^{-25}$)	increased hepatocyte MCM2 expression linked with fibrosis progression in HCV infection.[110]	Core-mediated enhanced MCM2 activity may contribute to fibrosis in HCV pathogenesis.
PTPN11	II (+)	Natural killer cell mediated cytotoxicity ($p = 3.64 \times 10^{-10}$); Jak-STAT signaling pathway ($p = 5.74 \times 10^{-5}$)	functions as a tumor suppressor in HCC and negatively regulates hepatic insulin action.[111,112]	increased PTPN11 levels may be associated with the absence of HCC progression in PA28γ−/−CoreTG.
RABEP1	III (−)	Endocytosis ($p = 2.08 \times 10^{-22}$)	interacts with NS3;[45] functions in early endocytic events and regulates mast cell activation.[113,114]	may possibly function in HCV propagation.
RB1	III (+)	Cell cycle ($p = 4.04 \times 10^{-20}$)	tumour suppressor, downregulated in HCC.[115,116]	increased RB1 levels in III consistent with the lack of HCC progression in the PA28γ−/−CoreTG mice.
TRADD	III (−)	Apoptosis ($p = 1.84 \times 10^{-15}$)	forms a complex with Core and TNFR1, implicated in HCV-induced chronic liver disease.[117]	decreased TRADD levels may contribute to the lack of IR and liver disease in PA28γ−/−CoreTG

[a]Host factors that were previously known to be associated with HCV pathogenesis and HCC and were mapped to various enriched KEGG pathways associated with the CoreTGvsWT, PA28γ−/−CoreTGvsWT, and PA28γ−/−CoreTGvsCoreTG PPI networks. [b]Data set I: CoreTGvsWT; Data set II: PA28γ−/−/CoreTGvsWT; Data set III: PA28γ−/−/CoreTGvsCoreTG; +: upregulated; −: downregulated.
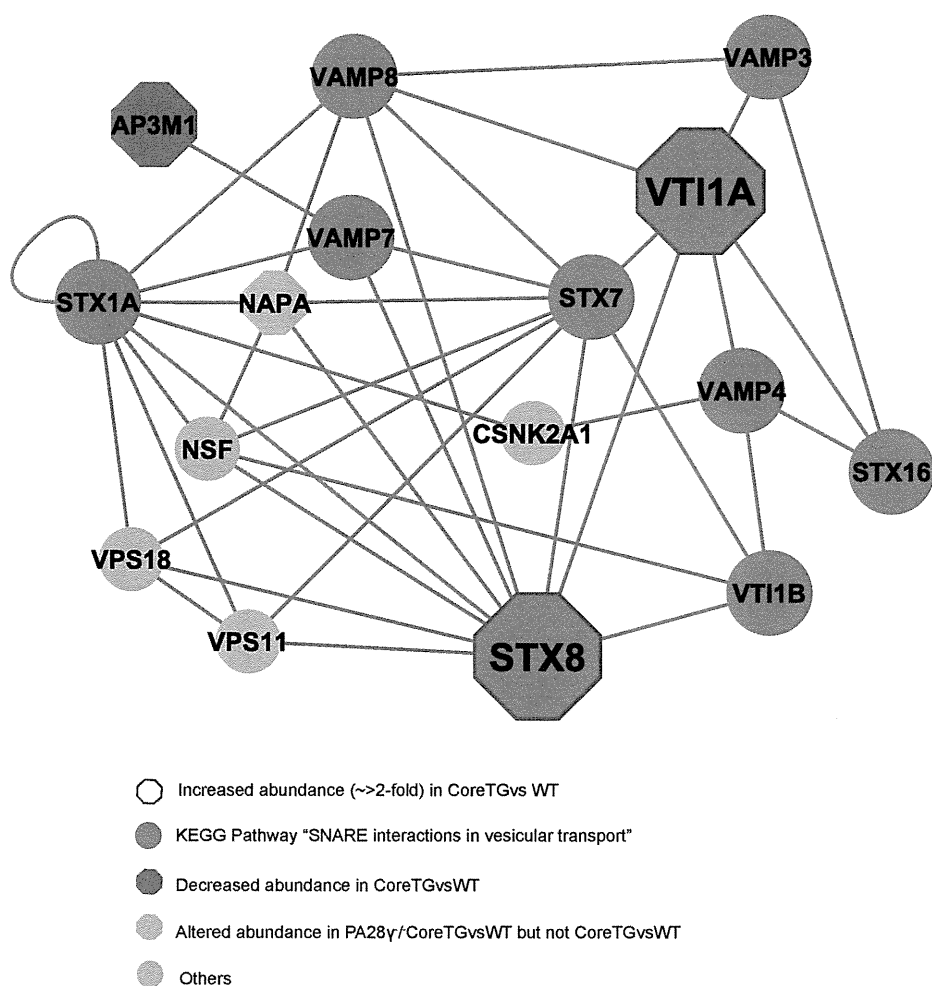
Figure 2. CoreTGvsWT SNARE network. Network illustration of the interactions between the PowerBlot identified differentially expressed proteins in CoreTGvsWT and human proteins mapped to the enriched KEGG pathway "SNARE interactions in vesicular transport". The node sizes differ for better clarity and do not reflect any topological attributes.

mechanism for the involvement of PA28γ in HCV propagation. Potentially, the suppression of PA28γ activity in PA28γ$^{-/-}$CoreTG mice may contribute to the overexpression of STX11 (and downregulation of USO1), thereby impairing the trafficking to the cell surface and consequently the release of the infectious HCV particles.

HCV has also been detected in the macrophages of certain infected patients,[64] suggesting that HCV may possibly infect the macrophages *in vivo* and regulate the STX11 (and USO1) expression to modulate the viral release and cytokine secretion.

EPS15 and RABEP1 (KEGG pathway "Endocytosis", $p = 2.08 \times 10^{-22}$) were decreased 2.11- and 2.74-fold, respectively, in PA28γ$^{-/-}$CoreTGvsCoreTG (Table 1, Table S5). EPS15 is an adaptor protein associated with the epidermal growth factor (EGF) signaling; it is localized to the clathrin-coated pits and functions in receptor-mediated endocytosis[65,66] and may play an important role in HCV pathogenesis (Table 2).

Immune System and Signal Transduction

HCV infection induces varied active and passive host immune responses such as the recognition of the infecting HCV RNA and proteins by the macrophages and the dendritic cells expressing Toll-like receptors (TLRs) and RIG-I-like receptors (RLRs). These events trigger the production of Type I interferons (IFN-α/β) and inflammatory cytokines in the infected hepatocytes, thereby initiating viral clearance. The ability to impair host immune responses contributes to the HCV persistence in the host.[67–72]

The PowerBlot analysis showed differentially expressed host proteins (IKBKG, MAP2K2, PPP3CA, SHC3, STAT1, TRADD) in PA28γ$^{-/-}$CoreTGvsCoreTG and their interacting partners that were mapped to one or more enriched KEGG pathways associated with the immune system (Table S5). IKBKG (IKK Gamma) is an antiapoptotic protein that is essential for NFKB activation and modulates TNF-mediated apoptosis.[73] IKBKG mutations are associated with immune deficiency phenotype (Table S7) and IKBKG may contribute to the activity of the hepatic carcinoma associated protein MAFIP in suppressing the proliferation of the cancer cells.[74] Additionally, specific deletion of IKBKG in the hepatocytes promotes NK-cell dependent liver damage.[75] Taken together, the elevated IKBKG abundance as observed in PA28γ$^{-/-}$CoreTGvsCoreTG (1.97-fold; Table 1) may contribute to the lack of HCC progression and reduced liver damage in the PA28γ$^{-/-}$CoreTG mice.

PPP3CA, MAP2K2, and SHC3 were mapped to the KEGG pathway "Natural killer cell mediated cytotoxicity" ($p = 1.67 \times 10^{-5}$; Table S5), the components of which function in the host immune response against the cancer cells and cells beset with pathogen infection.[76] PPP3CA levels were increased 12.94-fold,
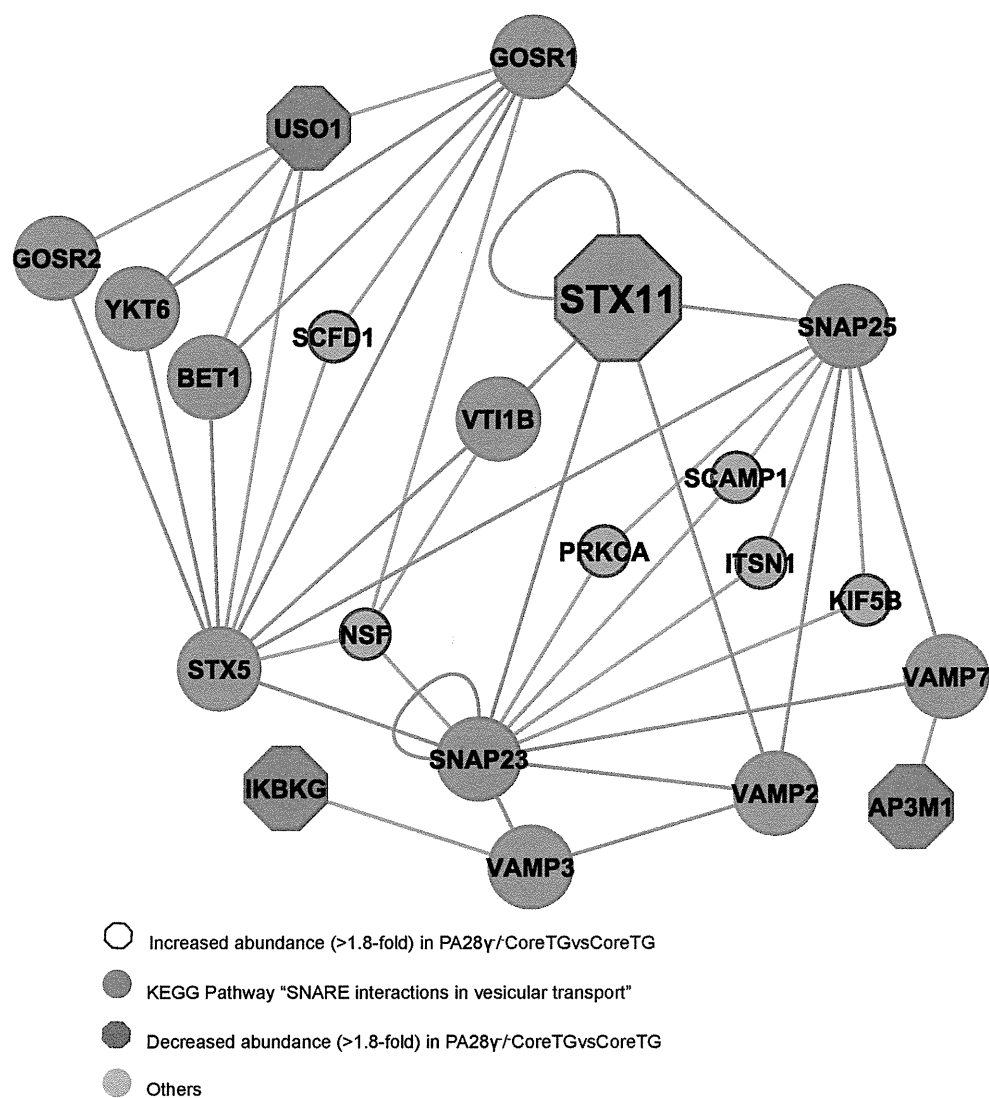
Figure 3. PA28$\gamma^{-/-}$CoreTGvsCoreTG SNARE network. Network illustration of the interactions between the PowerBlot identified differentially expressed proteins in PA28$\gamma^{-/-}$CoreTGvsCoreTG and human proteins mapped to the enriched KEGG pathway "SNARE interactions in vesicular transport". The node sizes differ for better clarity and do not reflect any topological attributes.

while MAP2K2 and SHC3 levels were suppressed 2.35-fold and 1.9-fold, respectively, in PA28$\gamma^{-/-}$CoreTGvsCoreTG (Table 1). These observations together with the increased STX11 abundance are consistent with the enhanced NK-cell mediated cytotoxicity that accompanies the STX11 overexpression.

PPP3CA is a tumor suppressor that negatively modulates the vascular endothelial growth factor (VEGF)-stimulated cell proliferation[77] and is downregulated in some cancerous cells.[78,79] PPP3CA was also mapped to the enriched KEGG pathways "VEGF signaling pathway" (p = 2.59 × 10^{-5}), "MAPK signaling pathway" (p = 2.37 × 10^{-16}) and "Wnt signaling pathway" (p = 1.048 × 10^{-10}; Table S5), which are implicated in the HCV infection and HCC. The 7.55-fold increase in PPP3CA abundance in PA28$\gamma^{-/-}$CoreTGvsCoreTG (Table 1) suggests that increased PPP3CA activity may significantly contribute to the lack of tumorigenesis and HCC progression in PA28$\gamma^{-/-}$CoreTG mice.

MAP2PK2 is a dual specificity MAP kinase that plays a critical role in the mitogen growth factor signal transduction. It is a key regulator of the TNF-α signaling and plays an important role in the tumor progression in certain cancers.[80]

Reduced MAP2K2 levels in the hepatocytes are implicated in enhanced apoptosis.[81] Therefore, the 2.66-fold decrease in MAP2K2 protein levels in PA28$\gamma^{-/-}$CoreTGvsCoreTG (Table 1) suggests that decreased MAP2K2 activity may contribute to the lack of HCC progression in PA28$\gamma^{-/-}$CoreTG mice. Our analysis thus identified potentially significant PA28γ-dependent roles of MAP2K2 and PPP3CA in a probable STX11-mediated regulation of NK cell activity in HCV pathogenesis.

MAP2K2, PPP3CA and SHC3 were also associated with the "Insulin signaling pathway" (p = 5.88 × 10^{-9}; Table S5), the disruption of which may contribute to insulin resistance (IR). IR is linked with steatosis, fibrosis progression and poor interferon-α response in HCV infection.[82,83] PA28γ contributes to hyperinsulinemia and IR in the CoreTG mice by impairing the insulin-signaling pathway through the suppression of Insulin receptor substrate 1 (IRS1) phosphorylation and increased tumor necrosis factor alpha (TNF-α) secretion.[12,84] The Powerblot analysis revealed that TRADD, which regulates TNF-α signaling as an antiapoptotic factor[85,86] and possibly functions in HCV pathogenesis (Table 2), was suppressed 2-fold in PA28$\gamma^{-/-}$CoreTGvsWT (Table 1).

Table 3. Summary of Proteins and Pathways Prioritized with TargetMine and Adjusted with the Help of Knowledge-Based Inputs for Experimental Investigation and/or Biomarker Discovery

(a) HCV replication and release

KEGG pathways	p-value	proteins[a]	data set[b]	knowledge-based evidence	refs
SNARE interactions in vesicular transport	0.023	VTI1A (+), STX8 (+)	I	regulation of the endosome-based membrane trafficking pathway implicated in HCV release	50, 52, 55
Steroid hormone biosynthesis	0.002	COMT (+)	I	COMT siRNA impairs HCV genotype 1b replication; functions in genotype 2a replication not known	50, 103
SNARE interactions in vesicular transport	0.003	STX11 (+)	III	modulation of specific components of the endosome-based membrane trafficking pathway implicated in HCV release; modulation of cytokine secretion in immune cells	50, 55, 57
Endocytosis	1.03×10^{-18}	CAV1 (+)	I	close homologue CAV2 associated with HCV replication complex; possible role in HCV replication	103

(b) steatosis, fibrosis, and hepatcarcinogenesis in HCV infection

KEGG pathways	p-value	proteins[a]	data set[b]	knowledge-based evidence	refs
Insulin signaling pathway	5.72×10^{-12}	AKT1 (−)	I	reduced AKT1 levels and phosophorylation associated with insulin resistance, which contributes to steatosis, fibrosis and HCC	118
Natural killer cell mediated cytotoxicity	1.67×10^{-5}	PPP3CA (+), MAP2K2 (−)	III	PPP3CA is a tumor suppressor with decreased levels in some cancers; PTPN1 is a tumor suppressor and regulates hepatic insulin signaling; decreased MAP2K2 levels in hepatocytes associated with enhanced apoptosis	78, 79, 81
Adherens junction	1.45×10^{-20}	CDH1 (−)	I	decreased CDH1 abundance associated with hepatocarcinogenesis and various cancers	106
Focal adhesion	5.57×10^{-12}	SHC1 (+)	II	loss of SHC1 function associated with tumor metastasis	119
Apoptosis	1.58×10^{-18}	BAX (+), CASP8 (+)	I	BAX interacts with NS5A and contributes to abnormal cytochrome c release in HCV infection; CASP8 activated in HCV infection	45, 90, 92, 93
Apoptosis	1.84×10^{-15}	TRADD (−)	III	antiapoptotic factor that forms a ternary complex containing Core, with likely functions in HCV-induced chronic liver disease	117
Chemokine signaling pathway	1.18×10^{-13}	ARRB1 (−)	I	interacts with PKM2, a key enzyme in glycolytic metabolism and cell growth and death in tumor cells	120

[a] +: upregulated. −: downregulated. [b] Data set I: CoreTGvsWT; Data set II: PA28$\gamma^{-/-}$CoreTGvsWT; Data set III: PA28$\gamma^{-/-}$CoreTGvsCoreTG.

Cell Adhesion

The Powerblot analysis revealed that host protein CSNK2B, the regulatory (beta) subunit of Casein Kinase II (CK2), was increased 1.88-fold in PA28$\gamma^{-/-}$CoreTGvsCoreTG (1.9-fold in PA28$\gamma^{-/-}$CoreTGvsWT). CK2 phosphorylates NS5A and regulates the production of infectious viral particles[87] and thus HCV pathogenesis (Table 2). CSNK2B was mapped to the enriched KEGG pathways "Adherens junction" ($p = 1.4 \times 10^{-13}$) and "Tight junction" ($p = 4.46 \times 10^{-7}$), some components of which are implicated in HCV entry and infection.[88]

SHC3 and TNR were decreased 1.9- and 4.62-fold, respectively, in PA28$\gamma^{-/-}$CoreTGvsCoreTG and were mapped to the enriched KEGG pathway "Focal adhesion" ($p = 3.56 \times 10^{-12}$; Table 1; Table S5), which regulates cell migration and adhesion to the extracellular matrix. Its deregulation is linked with tumor progression and possibly HCV propagation.[45] Previously, a Core interacting protein ENO1, associated with the focal adhesion, was identified as a novel regulator of HCV replication and release,[22] suggesting that SHC3 and TNR may play important roles in HCV pathogenesis.

Cell Growth and Death

Host cell apoptosis plays a critical role in HCV pathogenesis. The induction of apoptosis in the hepatocytes contributes to cell damage and fibrosis, whereas the induction of apoptosis in the peripheral blood mononuclear cells (PMBC), such as the T-cells, contributes significantly to the impaired immune response and HCV persistence in the host.[89−94] PA28γ is implicated in the cell cycle regulation, cell proliferation, and apoptosis[95−98] and likely plays a critical role in the manipulation of the cell cycle and apoptosis in HCV pathogenesis.

PPP3CA, TRADD, PRKAR2A, and IKBKG, with increased or decreased abundances in PA28$\gamma^{-/-}$CoreTGvsCoreTG, were mapped to KEGG pathway "Apoptosis" ($p = 1.84 \times 10^{-15}$; Table S5). PPP3CA was also mapped to "Oocyte meiosis" ($p = 9.84 \times 10^{-10}$; Table S5), associated with cell division. PPP3CA levels were highly elevated (12.94-fold) in PA28$\gamma^{-/-}$CoreTGvsCoreTG (Table 1), which may contribute to the accelerated cell death and the lack of tumor progression in PA28$\gamma^{-/-}$CoreTG mice.

PRKAR2A levels were decreased 1.88-fold in PA28$\gamma^{-/-}$CoreTGvsCoreTG (Table 1). PRKAR2A codes for a regulatory subunit of the cAMP dependent protein kinase (PKA), an important mediator of the cAMP signal transduction and elevated PRKAR2A expression is associated with an increased proliferation of the rat alveolar cells.[99] The suppression of PRKAR2A activity may therefore contribute to the lack of tumor proliferation in the PA28$\gamma^{-/-}$CoreTG mice.

Prioritization and Validation of the Novel Candidates for Their Role in HCV Replication and Release

Target prioritiszation using TargetMine is a simple process that involves uploading an initial list of candidates (in this instance the proteins in the CoreTGvsWT, PA28$\gamma^{-/-}$CoreTGvsWT, and PA28$\gamma^{-/-}$CoreTGvsCoreTG extended PPI networks) and estimating enriched biological themes associated with the input list.[16] Knowledge-based inputs may then be employed to further screen the proteins mapped to the top ranking significant associations to infer a manageable set of candidates. With the help of TargetMine, we previously investigated the significance of interactions between HCV Core and NS4B proteins and host factors in HCV infection and identified three novel regulators of HCV replication and propagation.[22]
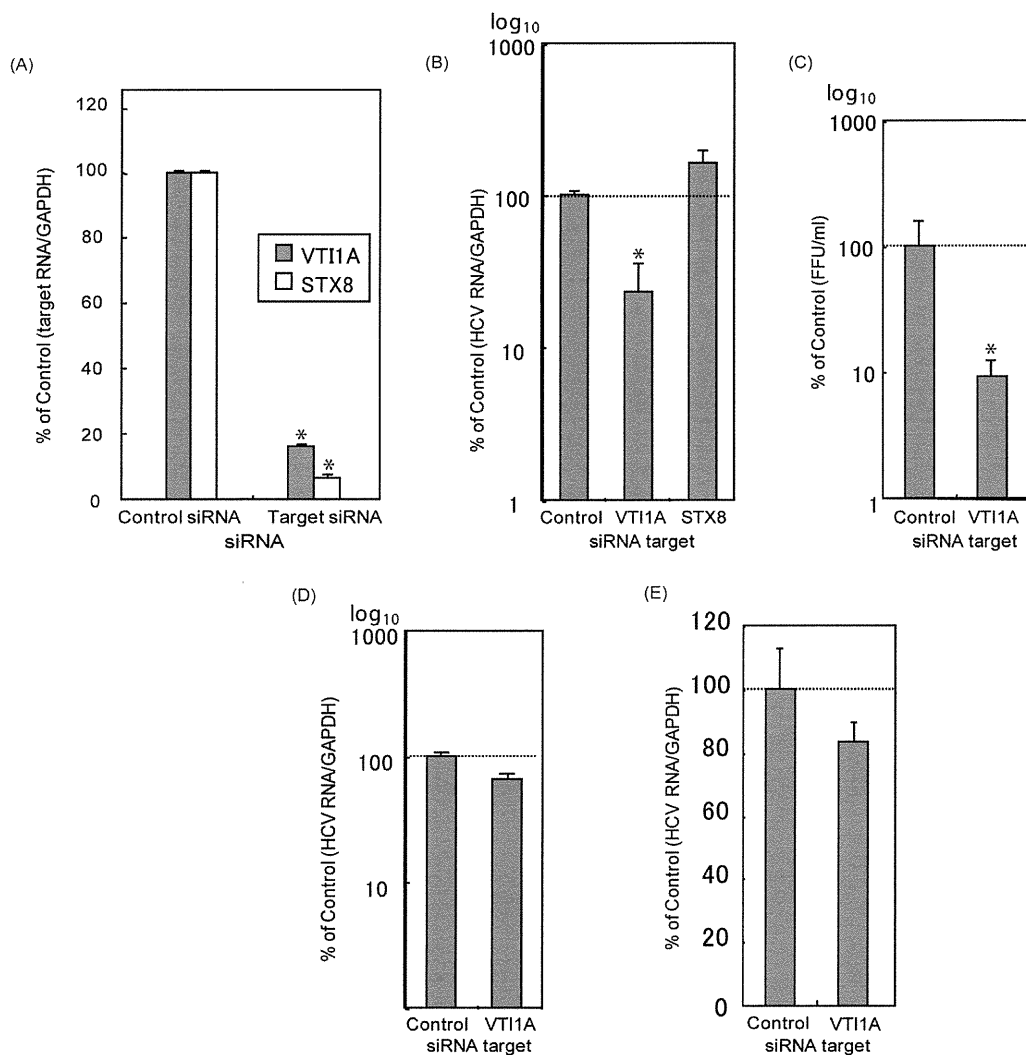
Figure 4. Effects of knockdown of candidate proteins on HCV propagation and replication. Host proteins VTI1A and STX8 were suppressed by RNAi (A) in Huh7OK1 cells infected with HCV JFH1 strain (genotype 2a; B, C, D) and in cells including subgenomic JFH1 replicon (E). The amounts of mRNA of the intracellular host proteins (A) and the supernatant viral RNA (B), viral titer (C), and intracellular viral RNA were estimated (D). The amount of the subgenomic viral RNA was also estimated (E). Each value was represented as percentage of the cells transfected with control siRNA; FFU: focus-forming units; $*$ $p < 0.01$.

Table 3 summarizes the prioritized candidates and pathways, all of which have been discussed above. Traditionally, viral and host proteins associated with the HCV lifecycle (internalization, replication, assembly, and release) have been preferred targets in the anti-HCV studies. The prioritized candidates and pathways in Table 3a fall within this category. In particular, our analysis suggested novel and potentially crucial roles of the host proteins VTI1A and STX8, which were elevated in CoreTG but not in PA28$\gamma^{-/-}$CoreTG, in the replication and/ or the release stages of the HCV lifecycle, therefore making these host proteins attractive targets for further investigation.

Because of the lack of a suitable model system for HCV infection, cell-culture-based systems for HCV RNA replication and infectious viral particle production have been extensively exploited to identify potential anti-HCV drug targets.[5,7−9] To further explore the roles of selected candidates in the HCV life cycle, we performed cellular assays to assess the impact of VTI1A and STX8 siRNA knockdowns on HCV replication and release. Since the HCV-production systems using the HCV JFH1 infectious strain (genotype 2a) isolates alone are capable of both efficient replication and the production of the infectious

HCV particles,[33,100] JFH1 was used to infect the Huh7OK1 cell line 24 h after transfection with each siRNA (see Materials and Methods). The infected cells were harvested after 72 h post-infection and the expression of each host protein was assessed by qRT-PCR (Figure 4A). Supernatant viral RNA and the viral titer were significantly decreased by the knockdown of VTI1A but were unaffected by the STX8 knockdown (Figure 4B,C). However, VTI1A and STX8A knockdowns had no effect on the intracellular viral RNA levels in the HCV infected cells (Figure 4D) or replicon cells derived from JFH1 strain (Figure 4E) or replicon cells derived from the Con1 (genotype 1b) strain (data not shown). These observations suggest that VTI1A regulates HCV propagation but not HCV replication.

The standard therapy of PEGylated interferon-α plus rebavirin treatment often results in severe side effects such as depression, flu-like symptoms, anemia, and fatigue that force the treatment to discontinue in affected patients, thus necessitating improved and combinatorial treatment strategies.[101,102] The genetic variability of HCV has led to increasing drug resistance. Thus, antivirals that target host proteins critical to viral pathogenesis, with a lower rate of mutation and

preferably with minimal adverse side effects, may provide attractive alternatives to HCV protein targets. VTI1A-deficient (knockout) mice are viable and fertile,[55] suggesting that the suppression of VTI1A activity may not have significantly undesirable side effects.

Inhibition of COMT (which was increased 2.71- and 2.96-fold in CoreTGvsWT and PA28$\gamma^{-/-}$CoreTG, respectively; Table 1) activity via siRNA knockdown was previously shown to result in a decreased HCV replication in cells infected with the Con1 strain.[103] To investigate other possible aspects (such as genotype specificity) of COMT function in the HCV life cycle, we assessed the impact of the COMT siRNA knockdown on HCV replication and release. COMT knockdown, however, had no effect on HCV propagation or replication in the cells including full length or subgenomic replicons derived from JFH1 or Con1 strains (data not shown). The discrepancy between our observations and those of Chan et al.[103] may be explained by the differences in the methodologies. We employed a transient transfection method to knockdown the selected targets to assess their roles in HCV replication and release, whereas Chan et al. employed a lentiviral expressing system for their experiments. Lentiviral mediated siRNA delivery is known to result in a persistent knockdown of gene expression,[104] and a persistent knockdown of COMT expression may be necessary to inhibit HCV replication *in vitro*.

That we were able to experimentally validate one of the three genes selected for experimental characterization reinforces the strengths of the elaborate PPI network-based approach to identify and prioritize suitable targets for experimental and therapeutic investigation.

CONCLUSIONS

By analyzing high-throughput proteomics data from transgenic mice expressing HCV Core protein in the liver (an *in vivo* model of HCV pathogenesis) with or without the knockout of the proteasome activator PA28γ, we highlighted the cellular responses to HCV infection *in vivo* and obtained further insights into the role of PA28γ in HCV infection.

We investigated the network context of the changes in the protein abundances by mapping them onto the human interactome with the help of the TargetMine data warehouse. The differentially expressed proteins that were integrated with the human interactome were observed to participate in compact and well connected cellular networks reflecting the ability of HCV to rapidly and efficiently react to the host responses to HCV infection. A functional analysis of the PPI networks highlighted the cellular pathways associated with vesicular transport, immune system, cellular adhesion, cell growth, and cell death among others that were most prominently influenced by Core and PA28γ in HCV infection. We also confirmed the previous observations that host factors such as AKT1, BAX, CASP8 CDH1, COMT, MCM2, PTPN11, and RB1 showed increased or decreased abundances in HCV infection. However, to the best of our knowledge, the precise molecular mechanisms of these factors' involvement in HCV pathogenesis and HCC were unknown, and our analysis suggests novel contributions of Core and PA28γ to the functions of these proteins.

Our observations were then used to prioritize potential candidates for the follow-up experimental investigations. Cellular assays based on siRNA knockdowns of selected candidates in the HCV infected and replicon cells validated VTI1A, a SNARE protein associated with vesicular transport,

which was upregulated in CoreTG but not in PA28$\gamma^{-/-}$CoreTG, as a novel regulator of HCV propagation but not replication. VTIA-deficient mice are largely indistinguishable from the normal mice except for minor growth retardation in a few instances; therefore, VTI1A is a promising novel candidate for anti-HCV therapy.

Our analysis not only builds on the present understanding of the Core-PA28γ interplay in HCV infection but also provides novel insights that would facilitate the clinical evaluation of proteomic changes associated with HCV pathogenesis. Our analysis also provides a generic framework for investigating large scale proteomic data. Such investigation may help identify common themes associated with different physiological conditions, especially pathogen (such as viral) infection and disease, and help develop effective broad spectrum strategies aimed at ameliorating pathogen infection and diseases.

ASSOCIATED CONTENT

Ⓢ Supporting Information

This material is available free of charge via the Internet at http://pubs.acs.org.

AUTHOR INFORMATION

Corresponding Author

*Tel: +81-72-641-9890. Fax: +81-72-641-9881. E-mail: kenji@nibio.go.jp.

Author Contributions

‖These authors contributed equally to this work.

Notes

The authors declare no competing financial interest.

REFERENCES

(1) Dubuisson, J. Hepatitis C virus proteins. *World J. Gastroenterol.* 2007, *13* (17), 2406–15.

(2) Moriishi, K.; Mochizuki, R.; Moriya, K.; Miyamoto, H.; Mori, Y.; Abe, T.; Murata, S.; Tanaka, K.; Miyamura, T.; Suzuki, T.; Koike, K.; Matsuura, Y. Critical role of PA28gamma in hepatitis C virus-associated steatogenesis and hepatocarcinogenesis. *Proc. Natl. Acad. Sci. U.S.A.* 2007, *104* (5), 1661–6.

(3) Myrmel, H.; Ulvestad, E.; Asjo, B. The hepatitis C virus enigma. *APMIS* 2009, *117* (5–6), 427–39.

(4) Tang, H.; Grise, H. Cellular and molecular biology of HCV infection and hepatitis. *Clin. Sci. (London)* 2009, *117* (2), 49–65.

(5) Moradpour, D.; Penin, F.; Rice, C. M. Replication of hepatitis C virus. *Nat. Rev. Microbiol.* 2007, *5* (6), 453–63.

(6) Simmonds, P.; Bukh, J.; Combet, C.; Deleage, G.; Enomoto, N.; Feinstone, S.; Halfon, P.; Inchauspe, G.; Kuiken, C.; Maertens, G.; Mizokami, M.; Murphy, D. G.; Okamoto, H.; Pawlotsky, J. M.; Penin, F.; Sablon, E.; Shin, I. T.; Stuyver, L. J.; Thiel, H. J.; Viazov, S.; Weiner, A. J.; Widell, A. Consensus proposals for a unified system of nomenclature of hepatitis C virus genotypes. *Hepatology* 2005, *42* (4), 962–73.

(7) De Francesco, R.; Migliaccio, G. Challenges and successes in developing new therapies for hepatitis C. *Nature* 2005, *436* (7053), 953–60.

(8) Kato, N.; Mori, K.; Abe, K.; Dansako, H.; Kuroki, M.; Ariumi, Y.; Wakita, T.; Ikeda, M. Efficient replication systems for hepatitis C virus using a new human hepatoma cell line. *Virus Res.* 2009, *146* (1–2), 41–50.

(9) Murray, C. L.; Rice, C. M. Hepatitis C: An unsuspected drug target. *Nature* 2010, *465* (7294), 42–4.

(10) Mori, Y.; Moriishi, K.; Matsuura, Y. Hepatitis C virus core protein: its coordinate roles with PA28gamma in metabolic abnormality and carcinogenicity in the liver. *Int. J. Biochem. Cell Biol.* 2008, *40* (8), 1437–42.

(11) Gao, G.; Luo, H. The ubiquitin-proteasome pathway in viral infections. *Can. J. Physiol. Pharmacol.* 2006, *84* (1), 5–14.

(12) Miyamoto, H.; Moriishi, K.; Moriya, K.; Murata, S.; Tanaka, K.; Suzuki, T.; Miyamura, T.; Koike, K.; Matsuura, Y. Involvement of the PA28gamma-dependent pathway in insulin resistance induced by hepatitis C virus core protein. *J. Virol.* 2007, *81* (4), 1727–35.

(13) Moriishi, K.; Okabayashi, T.; Nakai, K.; Moriya, K.; Koike, K.; Murata, S.; Chiba, T.; Tanaka, K.; Suzuki, R.; Suzuki, T.; Miyamura, T.; Matsuura, Y. Proteasome activator PA28gamma-dependent nuclear retention and degradation of hepatitis C virus core protein. *J. Virol.* 2003, *77* (19), 10237–49.

(14) Moriishi, K.; Shoji, I.; Mori, Y.; Suzuki, R.; Suzuki, T.; Kataoka, C.; Matsuura, Y. Involvement of PA28gamma in the propagation of hepatitis C virus. *Hepatology* 2010, *52* (2), 411–20.

(15) Suzuki, R.; Moriishi, K.; Fukuda, K.; Shirakura, M.; Ishii, K.; Shoji, I.; Wakita, T.; Miyamura, T.; Matsuura, Y.; Suzuki, T. Proteasomal turnover of hepatitis C virus core protein is regulated by two distinct mechanisms: a ubiquitin-dependent mechanism and a ubiquitin-independent but PA28gamma-dependent mechanism. *J. Virol.* 2009, *83* (5), 2389–92.

(16) Chen, Y. A.; Tripathi, L. P.; Mizuguchi, K. TargetMine, an integrated data warehouse for candidate gene prioritisation and target discovery. *PLoS One* 2011, *6* (3), e17844.

(17) Liu, M. C.; Akle, V.; Zheng, W.; Dave, J. R.; Tortella, F. C.; Hayes, R. L.; Wang, K. K. Comparing calpain- and caspase-3-mediated degradation patterns in traumatic brain injury by differential proteome analysis. *Biochem. J.* 2006, *394* (Pt 3), 715–25.

(18) Stark, C.; Breitkreutz, B. J.; Reguly, T.; Boucher, L.; Breitkreutz, A.; Tyers, M. BioGRID: a general repository for interaction datasets. *Nucleic Acids Res.* 2006, *34* (Database issue), D535–9.

(19) Turner, B.; Razick, S.; Turinsky, A. L.; Vlasblom, J.; Crowdy, E. K.; Cho, E.; Morrison, K.; Donaldson, I. M.; Wodak, S. J. iRefWeb: interactive analysis of consolidated protein interaction data and their supporting evidence. *Database (Oxford)* 2010, *2010*, baq023.

(20) Cline, M. S.; Smoot, M.; Cerami, E.; Kuchinsky, A.; Landys, N.; Workman, C.; Christmas, R.; Avila-Campilo, I.; Creech, M.; Gross, B.; Hanspers, K.; Isserlin, R.; Kelley, R.; Killcoyne, S.; Lotia, S.; Maere, S.; Morris, J.; Ono, K.; Pavlovic, V.; Pico, A. R.; Vailaya, A.; Wang, P. L.; Adler, A.; Conklin, B. R.; Hood, L.; Kuiper, M.; Sander, C.; Schmulevich, I.; Schwikowski, B.; Warner, G. J.; Ideker, T.; Bader, G. D. Integration of biological networks and gene expression data using Cytoscape. *Nat. Protoc.* 2007, *2* (10), 2366–82.

(21) Assenov, Y.; Ramirez, F.; Schelhorn, S. E.; Lengauer, T.; Albrecht, M. Computing topological parameters of biological networks. *Bioinformatics* 2008, *24* (2), 282–4.

(22) Tripathi, L. P.; Kataoka, C.; Taguwa, S.; Moriishi, K.; Mori, Y.; Matsuura, Y.; Mizuguchi, K. Network based analysis of hepatitis C virus Core and NS4B protein interactions. *Mol. Biosyst.* 2010, *6* (12), 2539–53.

(23) Ashburner, M.; Ball, C. A.; Blake, J. A.; Botstein, D.; Butler, H.; Cherry, J. M.; Davis, A. P.; Dolinski, K.; Dwight, S. S.; Eppig, J. T.; Harris, M. A.; Hill, D. P.; Issel-Tarver, L.; Kasarskis, A.; Lewis, S.; Matese, J. C.; Richardson, J. E.; Ringwald, M.; Rubin, G. M.; Sherlock, G. Gene ontology: tool for the unification of biology. The Gene Ontology Consortium. *Nat. Genet.* 2000, *25* (1), 25–9.

(24) Aoki-Kinoshita, K. F.; Kanehisa, M. Gene annotation and pathway mapping in KEGG. *Methods Mol. Biol.* 2007, *396*, 71–91.

(25) McKusick-Nathans Institute of Genetic Medicine, Johns Hopkins Medicine (Baltimore, MD) and National Center for Biotechnology Information, National Library of Medicine (Bethesda, MD), Online Mendelian Inheritance in Man, OMIM (TM). In 2010.

(26) Benjamini, Y.; Hochberg, Y. Controlling the false discovery rate-A practical and powerful approach to multiple testing. *J. R. Statist. Soc. B* 1995, *57* (1), 289–300.

(27) Noble, W. S. How does multiple testing correction work? *Nat. Biotechnol.* 2009, *27* (12), 1135–7.

(28) Linhart, C.; Halperin, Y.; Shamir, R. Transcription factor and microRNA motif discovery: the Amadeus platform and a compendium of metazoan target sets. *Genome Res.* 2008, *18* (7), 1180–9.

(29) Montgomery, S. B.; Griffith, O. L.; Sleumer, M. C.; Bergman, C. M.; Bilenky, M.; Pleasance, E. D.; Prychyna, Y.; Zhang, X.; Jones, S. J. ORegAnno: an open access database and curation system for literature-derived promoters, transcription factor binding sites and regulatory variation. *Bioinformatics* 2006, *22* (5), 637–40.

(30) Okamoto, T.; Omori, H.; Kaname, Y.; Abe, T.; Nishimura, Y.; Suzuki, T.; Miyamura, T.; Yoshimori, T.; Moriishi, K.; Matsuura, Y. A single-amino-acid mutation in hepatitis C virus NS5A disrupting FKBP8 interaction impairs viral replication. *J. Virol.* 2008, *82* (7), 3480–9.

(31) Pietschmann, T.; Lohmann, V.; Kaul, A.; Krieger, N.; Rinck, G.; Rutter, G.; Strand, D.; Bartenschlager, R. Persistent and transient replication of full-length hepatitis C virus genomes in cell culture. *J. Virol.* 2002, *76* (8), 4008–21.

(32) Kato, T.; Date, T.; Miyamoto, M.; Furusaka, A.; Tokushige, K.; Mizokami, M.; Wakita, T. Efficient replication of the genotype 2a hepatitis C virus subgenomic replicon. *Gastroenterology* 2003, *125* (6), 1808–17.

(33) Wakita, T.; Pietschmann, T.; Kato, T.; Date, T.; Miyamoto, M.; Zhao, Z.; Murthy, K.; Habermann, A.; Krausslich, H. G.; Mizokami, M.; Bartenschlager, R.; Liang, T. J. Production of infectious hepatitis C virus in tissue culture from a cloned viral genome. *Nat. Med.* 2005, *11* (7), 791–6.

(34) Cao, W.; Sun, B.; Feitelson, M. A.; Wu, T.; Tur-Kaspa, R.; Fan, Q. Hepatitis C virus targets over-expression of arginase I in hepatocarcinogenesis. *Int. J. Cancer* 2009, *124* (12), 2886–92.

(35) Tacke, R. S.; Tosello-Trampont, A.; Nguyen, V.; Mullins, D. W.; Hahn, Y. S. Extracellular hepatitis C virus core protein activates STAT3 in human monocyte/macrophage/dendritic cells via an IL-6 autocrine pathway. *J. Biol. Chem.* 2011, DOI: 10.1074/jbc.M110.217653 .

(36) Waris, G.; Turkson, J.; Hassanein, T.; Siddiqui, A. Hepatitis C virus (HCV) constitutively activates STAT-3 via oxidative stress: role of STAT-3 in HCV replication. *J. Virol.* 2005, *79* (3), 1569–80.

(37) Randall, G.; Panis, M.; Cooper, J. D.; Tellinghuisen, T. L.; Sukhodolets, K. E.; Pfeffer, S.; Landthaler, M.; Landgraf, P.; Kan, S.; Lindenbach, B. D.; Chien, M.; Weir, D. B.; Russo, J. J.; Ju, J.; Brownstein, M. J.; Sheridan, R.; Sander, C.; Zavolan, M.; Tuschl, T.; Rice, C. M. Cellular cofactors affecting hepatitis C virus infection and replication. *Proc. Natl. Acad. Sci. U.S.A.* 2007, *104* (31), 12884–9.

(38) Lin, W.; Kim, S. S.; Yeung, E.; Kamegaya, Y.; Blackard, J. T.; Kim, K. A.; Holtzman, M. J.; Chung, R. T. Hepatitis C virus core protein blocks interferon signaling by interaction with the STAT1 SH2 domain. *J. Virol.* 2006, *80* (18), 9226–35.

(39) Tsutsumi, T.; Suzuki, T.; Moriya, K.; Shintani, Y.; Fujie, H.; Miyoshi, H.; Matsuura, Y.; Koike, K.; Miyamura, T. Hepatitis C virus core protein activates ERK and p38 MAPK in cooperation with ethanol in transgenic mice. *Hepatology* 2003, *38* (4), 820–8.

(40) Nanda, S. K.; Herion, D.; Liang, T. J. The SH3 binding motif of HCV [corrected] NS5A protein interacts with Bin1 and is important for apoptosis and infectivity. *Gastroenterology* 2006, *130* (3), 794–809.

(41) Jacobs, J. M.; Diamond, D. L.; Chan, E. Y.; Gritsenko, M. A.; Qian, W.; Stastna, M.; Baas, T.; Camp, D. G., 2nd; Carithers, R. L., Jr.; Smith, R. D.; Katze, M. G. Proteome analysis of liver cells expressing a full-length hepatitis C virus (HCV) replicon and biopsy specimens of

posttransplantation liver from HCV-infected patients. *J. Virol.* 2005, 79 (12), 7558–69.

(42) Woodhouse, S. D.; Narayan, R.; Latham, S.; Lee, S.; Antrobus, R.; Gangadharan, B.; Luo, S.; Schroth, G. P.; Klenerman, P.; Zitzmann, N. Transcriptome sequencing, microarray, and proteomic analyses reveal cellular and metabolic impact of hepatitis C virus infection in vitro. *Hepatology* 2010, 52 (2), 443–53.

(43) Fujino, T.; Nakamuta, M.; Yada, R.; Aoyagi, Y.; Yasutake, K.; Kohjima, M.; Fukuizumi, K.; Yoshimoto, T.; Harada, N.; Yada, M.; Kato, M.; Kotoh, K.; Taketomi, A.; Maehara, Y.; Nakashima, M.; Enjoji, M. Expression profile of lipid metabolism-associated genes in hepatitis C virus-infected human liver. *Hepatol. Res.* 2010, 40 (9), 923–9.

(44) MacPherson, J. I.; Sidders, B.; Wieland, S.; Zhong, J.; Targett-Adams, P.; Lohmann, V.; Backes, P.; Delpuech-Adams, O.; Chisari, F.; Lewis, M.; Parkinson, T.; Robertson, D. L. An integrated transcriptomic and meta-analysis of hepatoma cells reveals factors that influence susceptibility to HCV infection. *PLoS One* 2011, 6 (10), e25584.

(45) de Chassey, B.; Navratil, V.; Tafforeau, L.; Hiet, M. S.; Aublin-Gex, A.; Agaugue, S.; Meiffren, G.; Pradezynski, F.; Faria, B. F.; Chantier, T.; Le Breton, M.; Pellet, J.; Davoust, N.; Mangeot, P. E.; Chaboud, A.; Penin, F.; Jacob, Y.; Vidalain, P. O.; Vidal, M.; Andre, P.; Rabourdin-Combe, C.; Lotteau, V. Hepatitis C virus infection protein network. *Mol. Syst. Biol.* 2008, 4, 230.

(46) Chazal, N.; Gerlier, D. Virus entry, assembly, budding, and membrane rafts. *Microbiol. Mol. Biol. Rev.* 2003, 67 (2), 226–37.

(47) Manes, S.; del Real, G.; Martinez, A. C. Pathogens: raft hijackers. *Nat. Rev. Immunol.* 2003, 3 (7), 557–68.

(48) Riethmuller, J.; Riehle, A.; Grassme, H.; Gulbins, E. Membrane rafts in host-pathogen interactions. *Biochim. Biophys. Acta* 2006, 1758 (12), 2139–47.

(49) Suzuki, T.; Suzuki, Y. Virus infection and lipid rafts. *Biol. Pharm. Bull.* 2006, 29 (8), 1538–41.

(50) Mannova, P.; Fang, R.; Wang, H.; Deng, B.; McIntosh, M. W.; Hanash, S. M.; Beretta, L. Modification of host lipid raft proteome upon hepatitis C virus replication. *Mol. Cell. Proteomics* 2006, 5 (12), 2319–25.

(51) Corless, L.; Crump, C. M.; Griffin, S. D.; Harris, M. Vps4 and the ESCRT-III complex are required for the release of infectious hepatitis C virus particles. *J. Gen. Virol.* 2010, 91 (Pt 2), 362–72.

(52) Lai, C. K.; Jeng, K. S.; Machida, K.; Lai, M. M. Hepatitis C virus egress and release depend on endosomal trafficking of core protein. *J. Virol.* 2010, 84 (21), 11590–8.

(53) Jahn, R.; Scheller, R. H. SNAREs—engines for membrane fusion. *Nat. Rev. Mol. Cell. Biol.* 2006, 7 (9), 631–43.

(54) Kreykenbohm, V.; Wenzel, D.; Antonin, W.; Atlachkine, V.; von Mollard, G. F. The SNAREs vti1a and vti1b have distinct localization and SNARE complex partners. *Eur. J. Cell Biol.* 2002, 81 (5), 273–80.

(55) Kunwar, A. J.; Rickmann, M.; Backofen, B.; Browski, S. M.; Rosenbusch, J.; Schoning, S.; Fleischmann, T.; Krieglstein, K.; Fischer von Mollard, G. Lack of the endosomal SNAREs vti1a and vti1b led to significant impairments in neuronal development. *Proc. Natl. Acad. Sci. U.S.A.* 2011, 108 (6), 2575–80.

(56) Mascia, L.; Langosch, D. Evidence that late-endosomal SNARE multimerization complex is promoted by transmembrane segments. *Biochim. Biophys. Acta* 2007, 1768 (3), 457–66.

(57) Offenhauser, C.; Lei, N.; Roy, S.; Collins, B. M.; Stow, J. L.; Murray, R. Z. Syntaxin 11 binds Vti1b and regulates late endosome to lysosome fusion in macrophages. *Traffic* 2011, 12, 762–73.

(58) Bryceson, Y. T.; Chiang, S. C.; Darmanin, S.; Fauriat, C.; Schlums, H.; Theorell, J.; Wood, S. M. Molecular mechanisms of natural killer cell activation. *J. Innate Immun.* 2011, 3 (3), 216–26.

(59) Arneson, L. N.; Brickshawana, A.; Segovis, C. M.; Schoon, R. A.; Dick, C. J.; Leibson, P. J. Cutting edge: syntaxin 11 regulates lymphocyte-mediated secretion and cytotoxicity. *J. Immunol.* 2007, 179 (6), 3397–401.

(60) Dabrazhynetskaya, A.; Ma, J.; Guerreiro-Cacais, A. O.; Arany, Z.; Rudd, E.; Henter, J. I.; Karre, K.; Levitskaya, J.; Levitsky, V. Syntaxin

11 marks a distinct intracellular compartment recruited to the immunological synapse of NK cells to co-localize with cytotoxic granules. *J. Cell. Mol. Med.* 2011, 16, 129–41.

(61) Gholam, C.; Grigoriadou, S.; Gilmour, K. C.; Gaspar, H. B. Familial haemophagocytic lymphohistiocytosis: advances in the genetic basis, diagnosis and management. *Clin. Exp. Immunol.* 2011, 163 (3), 271–83.

(62) How, P. C.; Shields, D. Tethering function of the caspase cleavage fragment of Golgi protein p115 promotes apoptosis via a p53-dependent pathway. *J. Biol. Chem.* 2011, 286 (10), 8565–76.

(63) Radulescu, A. E.; Mukherjee, S.; Shields, D. The Golgi protein p115 associates with gamma-tubulin and plays a role in Golgi structure and mitosis progression. *J. Biol. Chem.* 2011, 286 (24), 21915–26.

(64) Bouffard, P.; Hayashi, P. H.; Acevedo, R.; Levy, N.; Zeldis, J. B. Hepatitis C virus is detected in a monocyte/macrophage subpopulation of peripheral blood mononuclear cells of infected patients. *J. Infect. Dis.* 1992, 166 (6), 1276–80.

(65) Roxrud, I.; Raiborg, C.; Pedersen, N. M.; Stang, E.; Stenmark, H. An endosomally localized isoform of Eps15 interacts with Hrs to mediate degradation of epidermal growth factor receptor. *J. Cell Biol.* 2008, 180 (6), 1205–18.

(66) Salcini, A. E.; Chen, H.; Iannolo, G.; De Camilli, P.; Di Fiore, P. P. Epidermal growth factor pathway substrate 15, Eps15. *Int. J. Biochem. Cell Biol.* 1999, 31 (8), 805–9.

(67) Barnaba, V. Hepatitis C virus infection: a "liaison a trois" amongst the virus, the host, and chronic low-level inflammation for human survival. *J. Hepatol.* 2010, 53 (4), 752–61.

(68) Hiroishi, K.; Ito, T.; Imawari, M. Immune responses in hepatitis C virus infection and mechanisms of hepatitis C virus persistence. *J. Gastroenterol. Hepatol.* 2008, 23 (10), 1473–82.

(69) Kawai, T.; Akira, S. Toll-like receptor and RIG-I-like receptor signaling. *Ann. N.Y. Acad. Sci.* 2008, 1143, 1–20.

(70) Sklan, E. H.; Charuworm, P.; Pang, P. S.; Glenn, J. S. Mechanisms of HCV survival in the host. *Nat. Rev. Gastroenterol. Hepatol.* 2009, 6 (4), 217–27.

(71) Szabo, G.; Dolganiuc, A. Hepatitis C and innate immunity: recent advances. *Clin. Liver Dis.* 2008, 12 (3), 675–92.

(72) Taylor, D. R.; Silberstein, E. Innate immunity and hepatitis C virus: eluding the host cell defense. *Front. Biosci.* 2009, 14, 4950–61.

(73) Legarda-Addison, D.; Hase, H.; O'Donnell, M. A.; Ting, A. T. NEMO/IKKgamma regulates an early NF-kappaB-independent cell-death checkpoint during TNF signaling. *Cell Death Differ.* 2009, 16 (9), 1279–88.

(74) Ye, X.; Lu, H.; Huo, K.; Chen, D. Finding a novel interacting protein of the hepatic carcinoma related gene MIP: NF-kappaB essential modulator (NEMO). *Oncol. Rep.* 2011, 25 (1), 231–5.

(75) Beraza, N.; Malato, Y.; Sander, L. E.; Al-Masaoudi, M.; Freimuth, J.; Riethmacher, D.; Gores, G. J.; Roskams, T.; Liedtke, C.; Trautwein, C. Hepatocyte-specific NEMO deletion promotes NK/NKT cell- and TRAIL-dependent liver damage. *J. Exp. Med.* 2009, 206 (8), 1727–37.

(76) Cruz-Munoz, M. E.; Veillette, A. Do NK cells always need a license to kill? *Nat. Immunol.* 2010, 11 (4), 279–80.

(77) Wang, K.; Song, Y.; Chen, D. B.; Zheng, J. Protein phosphatase 3 differentially modulates vascular endothelial growth factor- and fibroblast growth factor 2-stimulated cell proliferation and signaling in ovine fetoplacental artery endothelial cells. *Biol. Reprod.* 2008, 79 (4), 704–10.

(78) Singh, A. P.; Bafna, S.; Chaudhary, K.; Venkatraman, G.; Smith, L.; Eudy, J. D.; Johansson, S. L.; Lin, M. F.; Batra, S. K. Genome-wide expression profiling reveals transcriptomic variation and perturbed gene networks in androgen-dependent and androgen-independent prostate cancer cells. *Cancer Lett.* 2008, 259 (1), 28–38.

(79) Ostenfeld, M. S.; Bramsen, J. B.; Lamy, P.; Villadsen, S. B.; Fristrup, N.; Sorensen, K. D.; Ulhoi, B.; Borre, M.; Kjems, J.; Dyrskjot, L.; Orntoft, T. F. miR-145 induces caspase-dependent and -independent cell death in urothelial cancer cell lines with targeting of an expression signature present in Ta bladder tumors. *Oncogene* 2010, 29 (7), 1073–84.

— 381 —

(80) Johansen, C.; Vestergaard, C.; Kragballe, K.; Kollias, G.; Gaestel, M.; Iversen, L. MK2 regulates the early stages of skin tumor promotion. *Carcinogenesis* **2009**, *30* (12), 2100−8.

(81) Wang, C.; Zhou, J.; Wang, S.; Ye, M.; Fan, G.; Zou, H.; Jiang, C. Shotgun approach based comparative proteomic analysis of levo-tetrahydropalmatine-induced apoptosis in hepatocytes. *Toxicol. Lett.* **2010**, *194* (1−2), 8−15.

(82) Del Campo, J. A.; Romero-Gomez, M. Steatosis and insulin resistance in hepatitis C: a way out for the virus? *World J. Gastroenterol.* **2009**, *15* (40), 5014−9.

(83) Douglas, M. W.; George, J. Molecular mechanisms of insulin resistance in chronic hepatitis C. *World J. Gastroenterol.* **2009**, *15* (35), 4356−64.

(84) Shintani, Y.; Fujie, H.; Miyoshi, H.; Tsutsumi, T.; Tsukamoto, K.; Kimura, S.; Moriya, K.; Koike, K. Hepatitis C virus infection and diabetes: direct involvement of the virus in the development of insulin resistance. *Gastroenterology* **2004**, *126* (3), 840−8.

(85) Cao, X.; Pobezinskaya, Y. L.; Morgan, M. J.; Liu, Z. G. The role of TRADD in TRAIL-induced apoptosis and signaling. *FASEB J.* **2011**, *25* (4), 1353−8.

(86) Zheng, L.; Bidere, N.; Staudt, D.; Cubre, A.; Orenstein, J.; Chan, F. K.; Lenardo, M. Competitive control of independent programs of tumor necrosis factor receptor-induced cell death by TRADD and RIP1. *Mol. Cell. Biol.* **2006**, *26* (9), 3505−13.

(87) Tellinghuisen, T. L.; Foss, K. L.; Treadaway, J. Regulation of hepatitis C virion production via phosphorylation of the NS5A protein. *PLoS Pathog.* **2008**, *4* (3), e1000032.

(88) Benedicto, I.; Molina-Jimenez, F.; Bartosch, B.; Cosset, F. L.; Lavillette, D.; Prieto, J.; Moreno-Otero, R.; Valenzuela-Fernandez, A.; Aldabe, R.; Lopez-Cabrera, M.; Majano, P. L. The tight junction-associated protein occludin is required for a postbinding step in hepatitis C virus entry and infection. *J. Virol.* **2009**, *83* (16), 8012−20.

(89) Bantel, H.; Schulze-Osthoff, K. Apoptosis in hepatitis C virus infection. *Cell Death Differ.* **2003**, *10* (Suppl 1), S48−58.

(90) Deng, L.; Adachi, T.; Kitayama, K.; Bungyoku, Y.; Kitazawa, S.; Ishido, S.; Shoji, I.; Hotta, H. Hepatitis C virus infection induces apoptosis through a Bax-triggered, mitochondrion-mediated, caspase 3-dependent pathway. *J. Virol.* **2008**, *82* (21), 10375−85.

(91) Fischer, R.; Baumert, T.; Blum, H. E. Hepatitis C virus infection and apoptosis. *World J. Gastroenterol.* **2007**, *13* (36), 4865−72.

(92) Hanafy, S. M.; Shehata, O. H.; Farahat, N. M. Expression of apoptotic markers BCL-2 and Bax in chronic hepatitis C virus patients. *Clin. Biochem.* **2010**, *43* (13−14), 1112−7.

(93) Joyce, M. A.; Walters, K. A.; Lamb, S. E.; Yeh, M. M.; Zhu, L. F.; Kneteman, N.; Doyle, J. S.; Katze, M. G.; Tyrrell, D. L. HCV induces oxidative and ER stress, and sensitizes infected cells to apoptosis in SCID/Alb-uPA mice. *PLoS Pathog.* **2009**, *5* (2), e1000291.

(94) Kondo, Y.; Machida, K.; Liu, H. M.; Ueno, Y.; Kobayashi, K.; Wakita, T.; Shimosegawa, T.; Lai, M. M. Hepatitis C virus infection of T cells inhibits proliferation and enhances fas-mediated apoptosis by down-regulating the expression of CD44 splicing variant 6. *J. Infect. Dis.* **2009**, *199* (5), 726−36.

(95) Anupam, R.; Datta, A.; Kesic, M.; Green-Church, K.; Shkriabai, N.; Kvaratskhelia, M.; Lairmore, M. D. Human T-lymphotropic virus type 1 p30 interacts with REGgamma and modulates ATM (ataxia telangiectasia mutated) to promote cell survival. *J. Biol. Chem.* **2011**, *286* (9), 7661−8.

(96) Mao, I.; Liu, J.; Li, X.; Luo, H. REGgamma, a proteasome activator and beyond? *Cell. Mol. Life Sci.* **2008**, *65* (24), 3971−80.

(97) Tian, M.; Xiaoyi, W.; Xiaotao, L.; Guosheng, R. Proteasomes reactivator REG gamma enchances oncogenicity of MDA-MB-231 cell line via promoting cell proliferation and inhibiting apoptosis. *Cell. Mol. Biol. (Noisy-le-Grand)* **2009**, *55* (Suppl), OL1121−31.

(98) Zannini, L.; Buscemi, G.; Fontanella, E.; Lisanti, S.; Delia, D. REGgamma/PA28gamma proteasome activator interacts with PML and Chk2 and affects PML nuclear bodies number. *Cell Cycle* **2009**, *8* (15), 2399−407.

(99) Samuelsen, J. T.; Schwarze, P. E.; Huitfeldt, H. S.; Thrane, E. V.; Lag, M.; Refsnes, M.; Skarpen, E.; Becher, R. Regulation of rat alveolar type 2 cell proliferation in vitro involves type II cAMP-dependent protein kinase. *Am. J. Physiol. Lung Cell. Mol. Physiol.* **2007**, *292* (1), L232−9.

(100) Bungyoku, Y.; Shoji, I.; Makine, T.; Adachi, T.; Hayashida, K.; Nagano-Fujii, M.; Ide, Y. H.; Deng, L.; Hotta, H. Efficient production of infectious hepatitis C virus with adaptive mutations in cultured hepatoma cells. *J. Gen. Virol.* **2009**, *90* (Pt 7), 1681−91.

(101) Lemon, S. M.; McKeating, J. A.; Pietschmann, T.; Frick, D. N.; Glenn, J. S.; Tellinghuisen, T. L.; Symons, J.; Furman, P. A. Development of novel therapies for hepatitis C. *Antiviral Res.* **2010**, *86* (1), 79−92.

(102) Lin, K. Development of novel antiviral therapies for hepatitis C virus. *Virol. Sin.* **2010**, *25* (4), 246−66.

(103) Chan, S. C.; Lo, S. Y.; Liou, J. W.; Lin, M. C.; Syu, C. L.; Lai, M. J.; Chen, Y. C.; Li, H. C. Visualization of the structures of the hepatitis C virus replication complex. *Biochem. Biophys. Res. Commun.* **2011**, *404* (1), 574−8.

(104) Dreyer, J. L. Lentiviral vector-mediated gene transfer and RNA silencing technology in neuronal dysfunctions. *Mol. Biotechnol.* **2011**, *47* (2), 169−87.

(105) Camm, E. J.; Martin-Gronert, M. S.; Wright, N. L.; Hansell, J. A.; Ozanne, S. E.; Giussani, D. A. Prenatal hypoxia independent of undernutrition promotes molecular markers of insulin resistance in adult offspring. *FASEB J.* **2011**, *25* (1), 420−7.

(106) Ning, B. F.; Ding, J.; Yin, C.; Zhong, W.; Wu, K.; Zeng, X.; Yang, W.; Chen, Y. X.; Zhang, J. P.; Zhang, X.; Wang, H. Y.; Xie, W. F. Hepatocyte nuclear factor 4 alpha suppresses the development of hepatocellular carcinoma. *Cancer Res.* **2010**, *70* (19), 7640−51.

(107) Niehof, M.; Borlak, J. EPS15R, TASP1, and PRPF3 are novel disease candidate genes targeted by HNF4alpha splice variants in hepatocellular carcinomas. *Gastroenterology* **2008**, *134* (4), 1191−202.

(108) Hussain, K. M.; Leong, K. L.; Ng, M. M.; Chu, J. J. The essential role of clathrin-mediated endocytosis in the infectious entry of human enterovirus 71. *J. Biol. Chem.* **2011**, *286* (1), 309−21.

(109) Helle, F.; Dubuisson, J. Hepatitis C virus entry into host cells. *Cell. Mol. Life Sci.* **2008**, *65* (1), 100−12.

(110) Marshall, A.; Rushbrook, S.; Morris, L. S.; Scott, I. S.; Vowler, S. L.; Davies, S. E.; Coleman, N.; Alexander, G. Hepatocyte expression of minichromosome maintenance protein-2 predicts fibrosis progression after transplantation for chronic hepatitis C virus: a pilot study. *Liver Transpl.* **2005**, *11* (4), 427−33.

(111) Bard-Chapeau, E. A.; Li, S.; Ding, J.; Zhang, S. S.; Zhu, H. H.; Princen, F.; Fang, D. D.; Han, T.; Bailly-Maitre, B.; Poli, V.; Varki, N. M.; Wang, H.; Feng, G. S. Ptpn11/Shp2 acts as a tumor suppressor in hepatocellular carcinogenesis. *Cancer Cell* **2011**, *19* (5), 629−39.

(112) Matsuo, K.; Delibegovic, M.; Matsuo, I.; Nagata, N.; Liu, S.; Bettaieb, A.; Xi, Y.; Araki, K.; Yang, W.; Kahn, B. B.; Neel, B. G.; Haj, F. G. Altered glucose homeostasis in mice with liver-specific deletion of Src homology phosphatase 2. *J. Biol. Chem.* **2010**, *285* (51), 39750−8.

(113) Rios, E. J.; Piliponsky, A. M.; Ra, C.; Kalesnikoff, J.; Galli, S. J. Rabaptin-5 regulates receptor expression and functional activation in mast cells. *Blood* **2008**, *112* (10), 4148−57.

(114) Stenmark, H.; Vitale, G.; Ullrich, O.; Zerial, M. Rabaptin-5 is a direct effector of the small GTPase Rab5 in endocytic membrane fusion. *Cell* **1995**, *83* (3), 423−32.

(115) Edamoto, Y.; Hara, A.; Biernat, W.; Terracciano, L.; Cathomas, G.; Riehle, H. M.; Matsuda, M.; Fujii, H.; Scoazec, J. Y.; Ohgaki, H. Alterations of RB1, p53 and Wnt pathways in hepatocellular carcinomas associated with hepatitis C, hepatitis B and alcoholic liver cirrhosis. *Int. J. Cancer* **2003**, *106* (3), 334−41.

(116) Laurent-Puig, P.; Zucman-Rossi, J. Genetics of hepatocellular tumors. *Oncogene* **2006**, *25* (27), 3778−86.

(117) Park, K. J.; Choi, S. H.; Koh, M. S.; Kim, D. J.; Yie, S. W.; Lee, S. Y.; Hwang, S. B. Hepatitis C virus core protein potentiates c-Jun N-terminal kinase activation through a signaling complex involving TRADD and TRAF2. *Virus Res.* **2001**, *74* (1−2), 89−98.

(118) Kawaguchi, T.; Yoshida, T.; Harada, M.; Hisamoto, T.; Nagao, Y.; Ide, T.; Taniguchi, E.; Kumemura, H.; Hanada, S.; Maeyama, M.;